AD-A069 559 OKLAHOMA STATE UNIV STILLWATER DEPT OF PHYSICS F/G 20/13
A STUDY OF DEFECTS PRODUCED BY THE IRRADIATION OF QUARTZ.(U)
MAR 79 L E HALLIBURTON, J J MARTIN F19628-77-C-0171
UNCLASSIFIED RADC-TR-79-33 NL

| OF |
AD
A069559

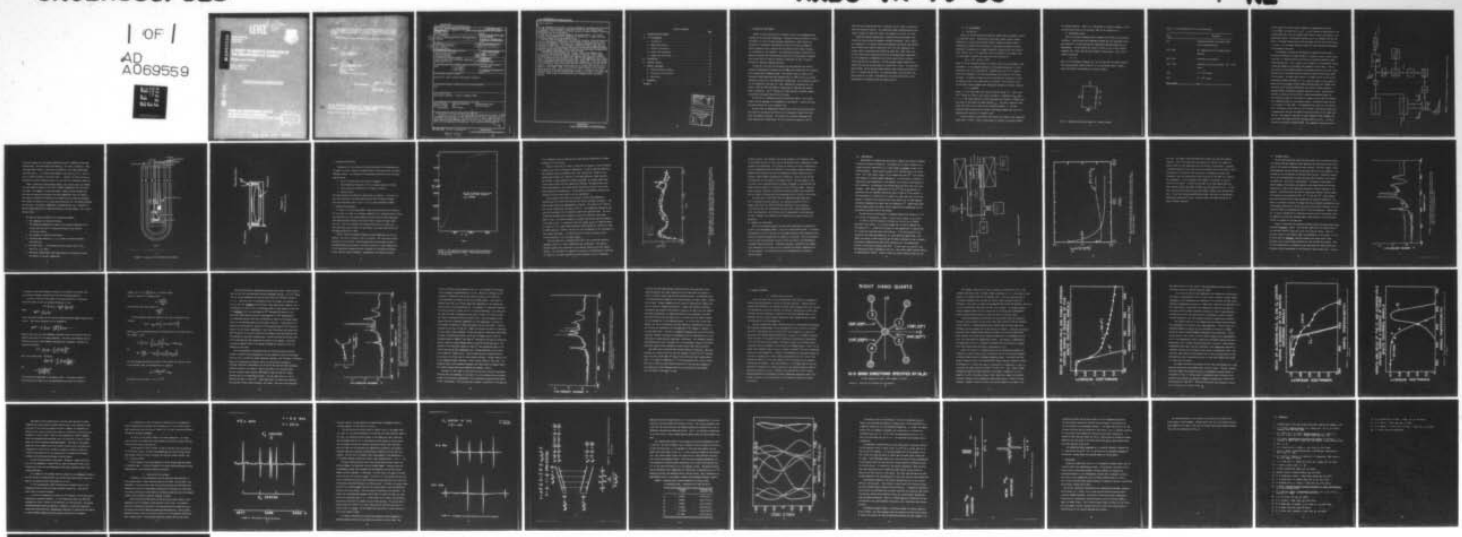

END
DATE
FILMED
7 -79
DDC

LEVEL II

AD A069559

A STUDY OF EFFECTS PRODUCED BY THE DEGRADATION OF QUARTZ

Oklahoma State University

Larry E. [illegible] Sherrow
Joel J. Martin
William A. Sibley

This report has been reviewed by the RADC Information Office (OI) and is releasable to the National Technical Information Service (NTIS). At NTIS it will be releasable to the general public, including foreign nations.

RADC-TR-79-33 has been reviewed and is approved for publication.

APPROVED:

ALTON F. [illegible]
Project Engineer

APPROVED:

ROBERT H. RAMSETT
Director
Solid State Sciences Division

FOR THE COMMANDER:

JOHN P. HUSS
Acting Chief, Plans Office

If your address has changed or if you wish to be removed from the RADC mailing list, or if the addressee is no longer employed by your organization, please notify RADC (OCSE), Hanscom AFB, MA 01731. This will assist us in maintaining an accurate distribution list.

Do not return this copy. Retain or destroy.

UNCLASSIFIED

SECURITY CLASSIFICATION OF THIS PAGE (When Data Entered)

REPORT DOCUMENTATION PAGE

READ INSTRUCTIONS BEFORE COMPLETING FORM

1. REPORT NUMBER: RADC-TR-79-33
2. GOVT ACCESSION NO.
3. RECIPIENT'S CATALOG NUMBER

4. TITLE (and Subtitle): A STUDY OF DEFECTS PRODUCED BY THE IRRADIATION OF QUARTZ.

5. TYPE OF REPORT & PERIOD COVERED: Interim Report. 15 May 77 - 15 May 78

6. PERFORMING ORG. REPORT NUMBER: N/A

7. AUTHOR(s): Larry E. Halliburton, Joel J. Martin, William A. Sibley

8. CONTRACT OR GRANT NUMBER(s): F 19628-77-C-0171

9. PERFORMING ORGANIZATION NAME AND ADDRESS: Oklahoma State University, Physics Department, Stillwater OK 74074

10. PROGRAM ELEMENT, PROJECT, TASK AREA & WORK UNIT NUMBERS: 61102F, 2306J127, J1

11. CONTROLLING OFFICE NAME AND ADDRESS: Deputy for Electronic Technology (RADC/ESM), Hanscom AFB MA 01731

12. REPORT DATE: March 1979

13. NUMBER OF PAGES: 56

14. MONITORING AGENCY NAME & ADDRESS (if different from Controlling Office): Same

15. SECURITY CLASS. (of this report): UNCLASSIFIED

15a. DECLASSIFICATION/DOWNGRADING SCHEDULE: N/A

16. DISTRIBUTION STATEMENT (of this Report)

Approved for public release; distribution unlimited.

17. DISTRIBUTION STATEMENT (of the abstract entered in Block 20, if different from Report)

Same

18. SUPPLEMENTARY NOTES

RADC Project Engineer: Alton K. Armington (ESM)

19. KEY WORDS (Continue on reverse side if necessary and identify by block number)

Quartz crystals
Radiation damage
Q^{-1} Measurements
Infrared absorption
ESR
Electrolysis
Aluminum-hole center
Electron center

20. ABSTRACT (Continue on reverse side if necessary and identify by block number)

During the first year of this project we have developed and tested a system for measuring the acoustic loss in 5MHz fifth overtone AT cut resonators by the logarithmic decrement method. The acoustic loss of a Sawyer swept Electronic Grade sample has been measured from 5 to 300 K in the as received condition and after two room temperature irradiations. The irradiation shifted (Cont'd)

DD FORM 1 JAN 73 1473 EDITION OF 1 NOV 65 IS OBSOLETE

UNCLASSIFIED

SECURITY CLASSIFICATION OF THIS PAGE (When Data Entered)

400 790

Item 20 (Cont'd)

the low temperature loss peak to a lower temperature, introduced new loss peaks at 100K and 125K and removed a large peak at 240K that was present before irradiation. The Q^{-1} studies are being continued on Sawyer Premium Q resonators fabricated from the D14-45 series.

We have set up a sweeping system to electrolyze quartz. Our current studies involve sweeping in an atmosphere of gettered Ar. Several runs have also been carried out in the presence of H_2.

We have used low temperature (liquid He and liquid N_2) infrared absorption scans to investigate the effects of our sweeping on Sawyer Electronic Grade and Premium Q material. Our results are in general agreement with those reported by the RADC group. The oscillator strength for the OH bands has been estimated and used to determine the H^+ content of Electronic Grade and Premium Q material. Low temperature (80K) irradiations have been found to enhance the 3306 cm^{-1} band at the expense of the 3367 cm^{-1} band.

Radiation-produced trapped hole, trapped electron and hydrogen atom centers have been studied by magnetic resonance techniques. When a sample is irradiated at 77K Al-hole centers and hydrogen atom centers are produced. The H^o centers were found to anneal near 120K; at this temperature the Al-hole center concentration was reduced by about 50%. Above 120K, the Al-hole concentration decreases slowly with increasing anneal temperature. For room temperature irradiations, the Al-hole center and two electron centers (E_2' and E_4') are observed. The two electron centers anneal out at around 410K and the Al-hole center at around 500K - 550K. As the Al-hole center decays, the E_1' electron center grows in with a peak concentration at 550K. It anneals out by 625K. An extensive study of the E_4' center has been carried out in order to determine the role this center plays in the stabilization of hydrogen within the quartz lattice.

TABLE OF CONTENTS

I. INTRODUCTION AND SUMMARY

Quartz is used extensively for frequency control in telecommunications systems and for precision timekeeping. Radiation hardness assurance of quartz oscillators is vital for many aerospace applications. This project was initiated to investigate the macroscopic effects of radiation damage on quartz resonators and to identify the microscopic defects which influence the performance of the resonator. By combining microscopic studies such as magnetic resonance and infrared spectroscopy with the macroscopic Q measurements which directly relate to resonator performance we hope to develop methods for radiation hardness assurance.

During the first year of this project we have developed and tested a system for measuring the acoustic loss in 5MHz fifth overtone AT cut resonators by the logarithmic decrement method. The acoustic loss of a Sawyer swept Electronic Grade sample has been measured from 5 to 300 K in the as received condition and after two room temperature irradiations. The irradiation shifted the low temperature loss peak to a lower temperature, introduced new loss peaks at 100K and 125K and removed a large peak at 240K that was present before irradiation. The Q^{-1} studies are being continued on Sawyer Premium Q resonators fabricated from the D14-45 series.

We have set up a sweeping system to electrolyze quartz. Our current studies involve sweeping in an atmosphere of gettered Ar. Several runs have also been carried out in the presence of H_2.

We have used low temperature (liquid He and liquid N_2) infrared absorption scans to investigate the effects of our sweeping on Sawyer Electronic Grade and Premium Q material. Our results are in general agreement with those reported by the RADC group (1). The oscillator strength for the OH

bands has been estimated and used to determine the H^+ content of Electronic Grade and Premium Q material. Low temperature (80K) irradiations have been found to enhance the 3306 cm^{-1} band at the expense of the 3367 cm^{-1} band.

Radiation-produced trapped hole, trapped electron and hydrogen atom centers have been studied by magnetic resonance techniques. When a sample is irradiated at 77 K Al-hole centers and hydrogen atom centers are produced. The H° centers were found to anneal near 120 K; at this temperature the Al-hole center concentration was reduced by about 50%. Above 120 K, the Al-hole concentration decreases slowly with increasing anneal temperature. For room temperature irradiations, the Al-hole center and two electron centers (E_2' and E_4') are observed. The two electron centers anneal out at around 410 K and the Al-hole center at around 500 K - 550 K. As the Al-hole center decays, the E_1' electron center grows in with a peak concentration at 550 K. It anneals out by 625 K. An extensive study of the E_4' center has been carried out in order to determine the role this center plays in the stabilization of hydrogen within the quartz lattice.

II. Q^{-1} MEASUREMENTS

A. Introduction

Fraser (2) has extensively reviewed the earlier work on anelastic effects in crystalline quartz. Anelasticity arises when a defect cannot respond instantly to a step function applied stress, instead the defect relaxes exponentially towards its new situation. Since Berry and Nowick (3) have discussed the response for a single relaxation process we will only outline their results here. If a sinusoidal stress is applied to the sample, then the phase angle δ between the stress and strain is given by

$$\tan \delta = Q^{-1} = D\omega\tau/(1 + \omega^2\tau^2)$$

where Q^{-1} is the internal friction or acoustic loss, D is the strength of the relaxation, ω is the angular frequency of the applied stress and τ is the relaxation time of the loss process. Although a plot of Q^{-1} vs ω gives a curve with a maximum at D/2, most measurements are carried out at a fixed frequency. In quartz, we made use of its piezoelectric properties to drive the sample in one of its normal modes of vibration. The relaxation time, τ of the defect usually depends upon temperature through an Arrhenius relation

$$\tau = \tau_o \exp(E/kT)$$

where τ_o is the "jump time" and E the activitation energy (4). Then a plot of Q^{-1} versus T at fixed ω will yield a maximum at a temperature T_{max} where $\omega\tau = 1$. The elastic modulus, M, which determines the resonant frequency will also shift as the sample is warmed through T_{max}. For quartz resonators this effect will show up as a shift in the resonant frequency, f. Thus any radiation-induced change in the acoustic loss versus temperature curve for a resonator will show up as a frequency shift.

A quartz resonator will usually have several loss peaks in the temperature range from 4 to 500 K. Some of these peaks are shifted or new ones produced

by ionizing radiation. Table I is a modification of Fraser's summary of loss characteristics found in 5th overtone 5 MHZ AT cut resonators.(5)

B. Measurement System

There are several techniques used to measure the acoustic loss in quartz resonators. These include the transmission method and the logarithmic decrement method (2). We have selected the logarithmic decrement method for our measurements. In this method the crystal is driven at its series resonant frequency for a short time and then allowed to freely decay. The Q of the crystal is given by

$$Q = \pi f \tau$$

where f is the resonant frequency and τ is the time that the signal from the free funning crystal takes to fall to e^{-1} of its initial value. Figure 1 gives the usually circuit model for a quartz crystal.

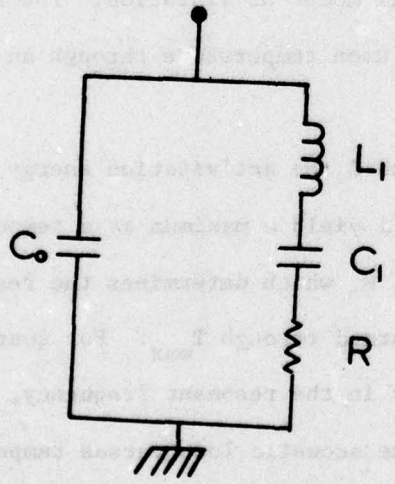

Fig. 1. Simplified electrical analog for a quartz crystal.

Table I. Loss Characteristics of AT cut Resonators.

T_{Max}	Mechanism
20K	Interaction between the resonant mode and the thermal phonons.
50K & 140K	Na^{+} compensating an Al^{3+} substitutional impurity.
85K & 140K	Produced by electrolysis.
100K & 130K	Produced by ionizing radiation: Al^{3+} - hole center.
105K	Li^{+} - Al^{3+} center
210K	K^{+} - Al^{3+} center
250K to 500K	OH

In this model the series resonant frequency is approximately given by $f = 1/2\pi\sqrt{L_1C_1}$ and the Q by $Q = \omega L_1/R$. C_o will include the capacitance of the crystal mount and, also, the coaxial cable used to connect the crystal to the measurement system. The parallel reactance due to C_o (perhaps 170Ω when the cable is included) shunts both the driving signal and the free running signal to ground. This low shunt reactance lowers the input impedance requirements of the detector circuitry.

In designing our system it was decided to measure the decay time, τ, by using the decaying DC output from an r.f. detector to gate a digital timer. Since the r.f. detector must be very linear we eventually adopted a super-heterodyne approach. Fig. 2 shows a block diagram of the measurement system. A detailed schematic is included in the appendix of this report. The r.f. gate circuit and the MOSFET amplifier are mounted directly at the top of the cryostat so as to minimize the shunt reactance caused by the coaxial leads to the crystal. The basic gate circuit is a simplification of the circuit described by Spencer and Smith (6). The amplified signal is heterodyned to 455kHz with an integrated circuit double balanced mixer and a stable local oscillator which operates 455kHz above the resonant crystal frequency. A standard 455kHz intermediate frequency amplifier is used. The precision detector is basically the fast AC/DC converter described by Dobkin (7). The integrating capacitor was changed to a small value so that the detector would respond properly to the decaying signal. The detector works well up to a frequency of about 1MHz. A DC amplifier with a gain of 10 is used to boost the detector output into the 5 to 10V range. The overall system gain is approximately 65db and the system is linear to within 1% for inputs less than 3mV. The output is then fed to a dual comparator which compares the output level with upper and lower switching levels V_u and V_l. V_u and V_l are set by a precision voltage divider. The comparator outputs are fed to

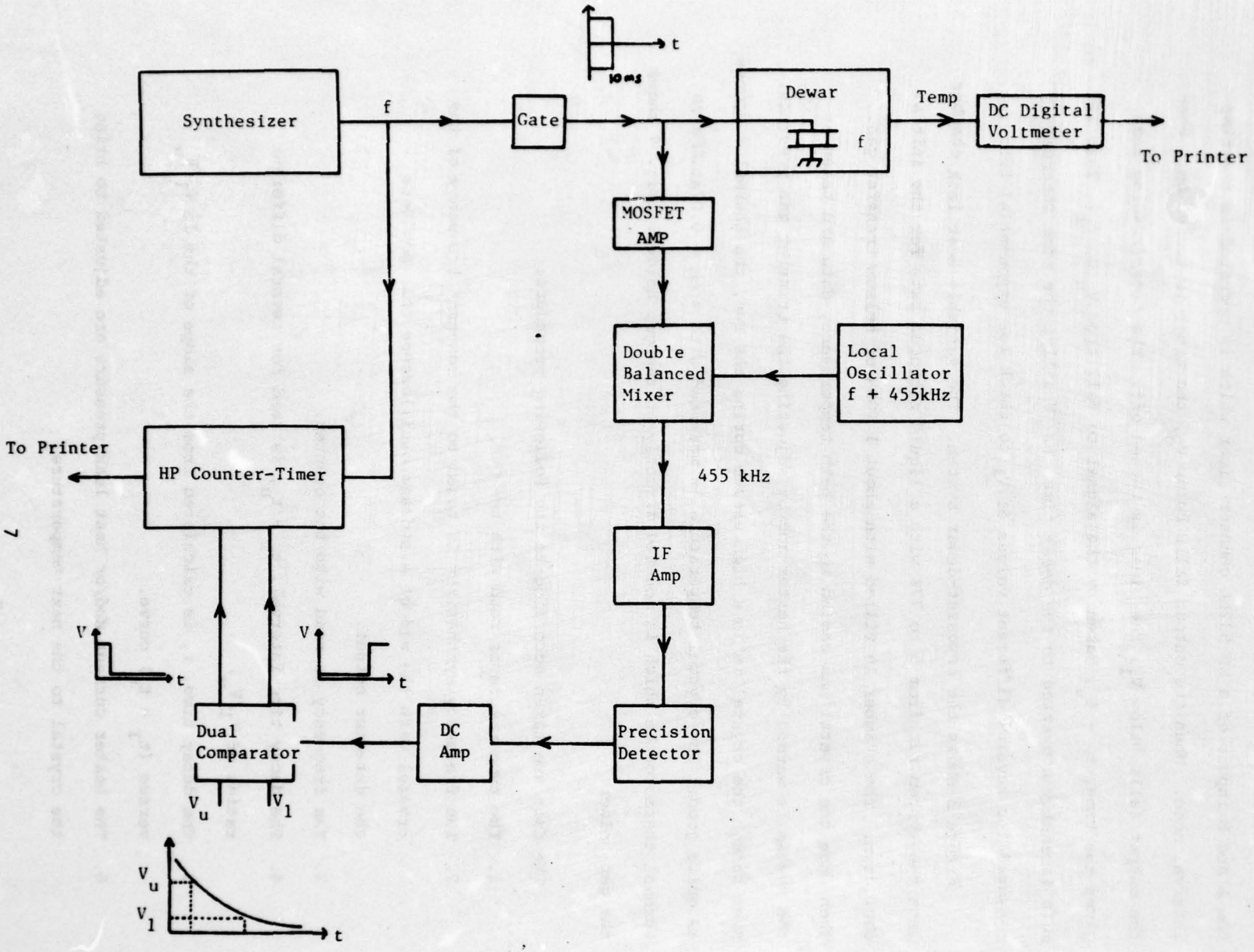

FIGURE 2. A block diagram of our Q^{-1} measurement system is shown.

the A and B inputs of a HP 5326A counter-timer which is operated in the time interval mode. When the output falls below V_u, the timer is turned on. When the output falls below V_l, the timer is turned off. The timer reading then gives the time, $t_l - t_u$, taken by the signal to fall from V_u to V_l. This result is easily converted to the decay time, τ. Usually, the time interval is measured for several different values of V_l to check for exponential behavior.

Figure 3 shows the cryostat-dewar system. The variable heat leak chamber lets the system run from 5 to 77K with a liquid nitrogen bath for the initial cool down. The chamber is filled with about 1 TORR of helium transfer gas. Then once the crystal has cooled to the bath temperature, data are taken as the system is warmed by the heater and by adjusting the transfer gas pressure. Even though the crystal is in a high vacuum during the run, the thermal response is quite good. The crystal temperature is measured with a Au + 0.07at.%Fe vs chromel thermocouple which is mounted directly on the gap holder. Fig. 4 shows the gap holder.

The data are taken according to the following procedure:

1. The temperature is read with the DVM.
2. The frequency synthesizer is tuned to the resonant frequency of the crystal with the aid of a storage oscilloscope that monitors the detector output.
3. The frequency is read with the counter.
4. The decay time interval, $t_l - t_u$, is read for several different ratios of V_l/V_u.
5. The decay time, τ, is calculated from the slope of the $\ln V_l/V_u$ versus $(t_l - t_u)$ curve.
6. The heater current and/or heat leak pressure are adjusted to bring the crystal to the next temperature.

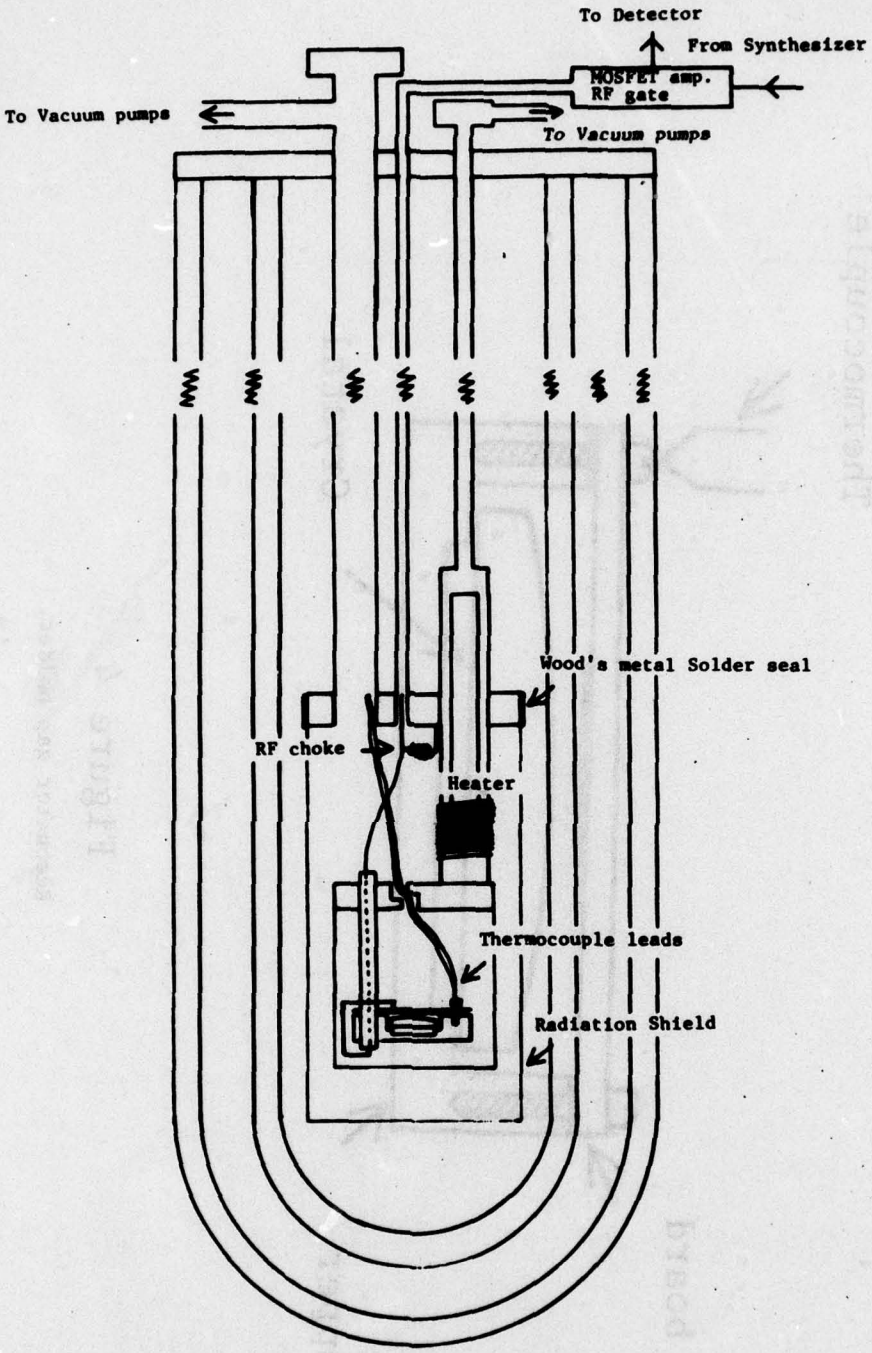

Figure 3

FIGURE 3. Cryostat for the acoustic loss system.

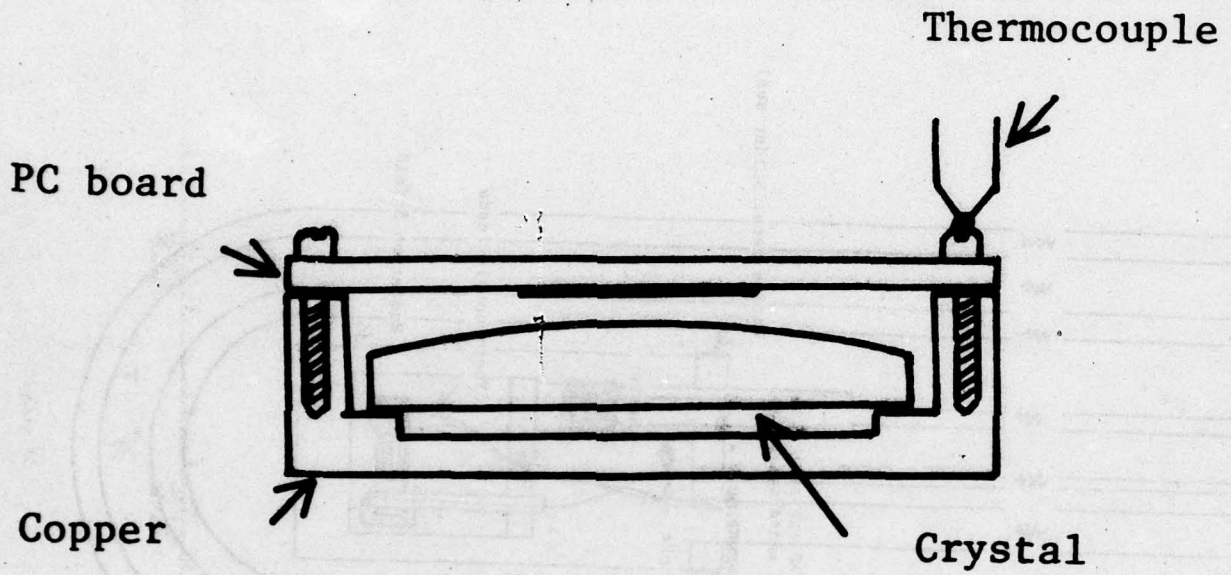

Figure 4

Resonator gap holder.

C. Resonator Fabrication

Resonators for this project are being fabricated by K-W Manufacturing of Prague, OK from a variety of lumbered pure Z growth quartz bars of several different grades. The resonators are fabricated according to the following specifications:

1. AT cut circular plate 0.60 inches in diameter.
2. 1MHz fundamental frequency, for 5th overtone operation at 5MHz.
3. Plano-convex lens shape with a 10 diopter curvature.
4. Optical finish.

The specifications are similar to those given by Fraser(2). Initially, we have four resonators each fabricated from the D14-45D Sawyer Premium Q bars that were swept with Li, Na, or K by Dr. Alton Armington at RADC.

D. Results and Discussion

In order to test the measurement system we have carried out a series of Q^{-1} runs from 5 to 300K on a resonator supplied by Mr. Ferdinand Euler of RADC. This resonator is a 5th overtone 5MHz plano-convex AT cut blank fabricated from Sawyer Research Products Electronic Grade Li doped and swept quartz bar B-3A. After the resonator was cleaned ultrasonically, rinsed with distilled water and air dried, it was mounted in the gap holder and the Q^{-1} was measured from 5K to 320K.

Figure 5 shows the resonant frequency versus temperature for this resonator. The curve is typical of AT cut crystals. The curve shows discontinuities at 32K and 194K. These discontinuities are probably caused by interfering modes which couple to the main vibration at these temperatures. In the logarithmic decrement method, we measure the synthesizer frequency rather than the crystal frequency. Consequently, the overall precision

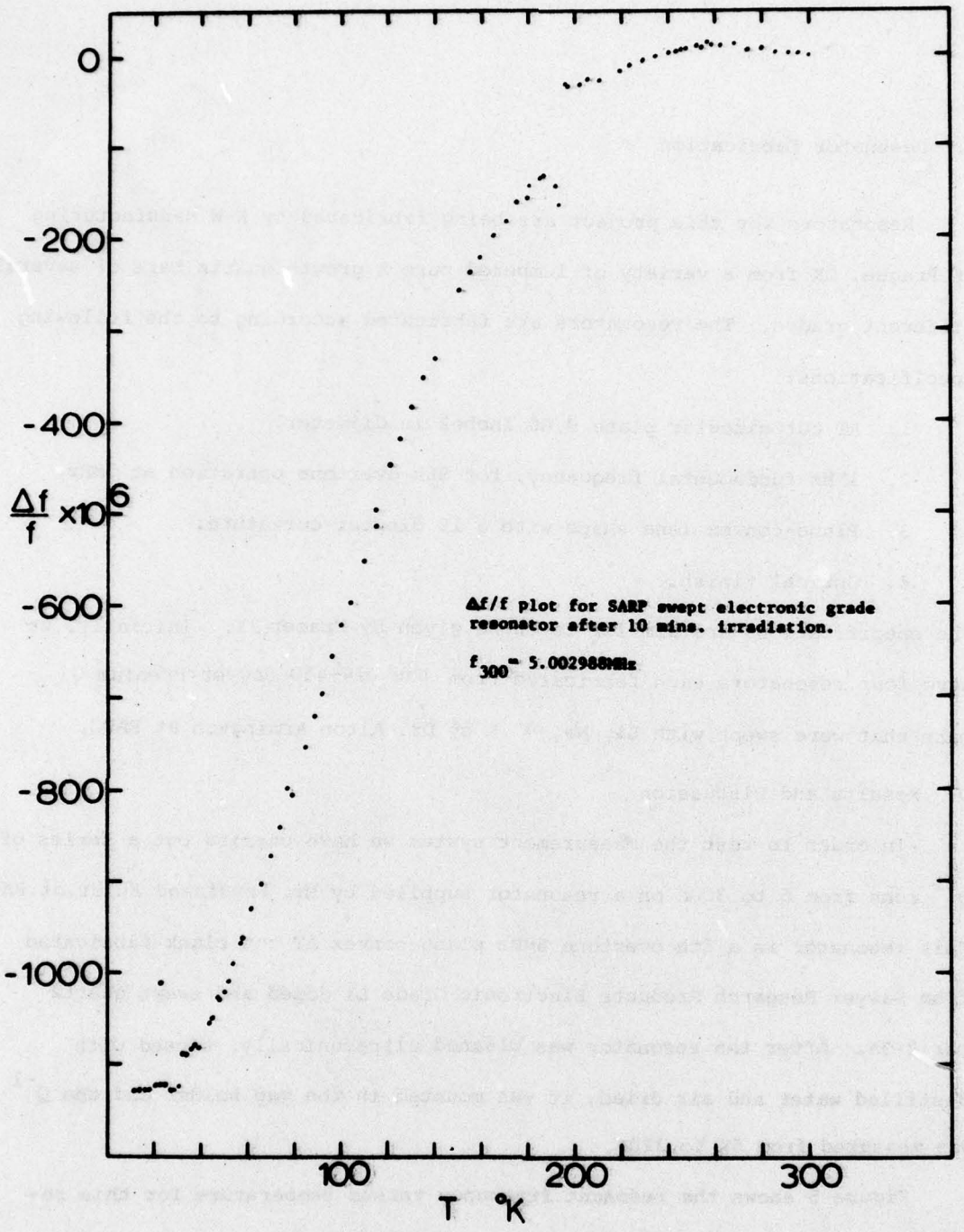

Figure 5

FIGURE 5. The fractional frequency shift versus temperature for an AT cut resonator is shown. Interfering modes appear at 32K and 194K.

of the frequency curve is less than one could obtain by measuring the output frequency of an oscillator.

Figure 6 shows the Q^{-1} versus T curves for the crystal in the as-received condition and for two successive irradiations. In the as-received condition, the resonator shows loss peaks at 40K, 170K, and at 235K. Except for the coupled mode problem, our results on this swept Electronic Grade resonator are similar to those reported by Capone, et al.(8) on a Sawyer swept Electronic Grade crystal that was commerically mounted. We observe some interfering mode behavior, but we have usually been able to tune it out by carefully adjusting the synthesizer. The differences are probably caused by the different crystal holder used in the two experiments.

This resonator was given two successive 5 minute room temperature irradiations with 1.5MeV electrons from the OSU van de Graaf accelerator. The beam current density was approximately $2.4\mu A/cm^2$. The curves of Q^{-1} versus T for the two irradiations are shown in Fig. 6. The irradiation lowered the 40K and 170K loss peaks, and it completely removed the 235K loss peak. The first irradiation produced new loss peaks at about 25K, 100K and a very sharp peak at 257K. The second irradiation increased the new 25K peak and produced a new peak at 125K. It should be noted that Capone, et al.(8) observed almost no change in Q^{-1} in their swept Electronic Grade crystal for a 1Mrad (Si) dose of 10MeV electrons, however, the dose for each irradiation in our experiment is much longer than 1Mrad. It should also be noted that no visible coloration was observed in our irradiated sample.

The loss peak that is observed below 50K in the as-received condition apparently shifts to a lower temperature upon irradiation. This peak is probably caused by an interaction of the applied vibration with the thermal phonons. The increased low temperature loss which we observed upon irradiation is similar to the result reported by Jones and Brown (9) for x-irradiated

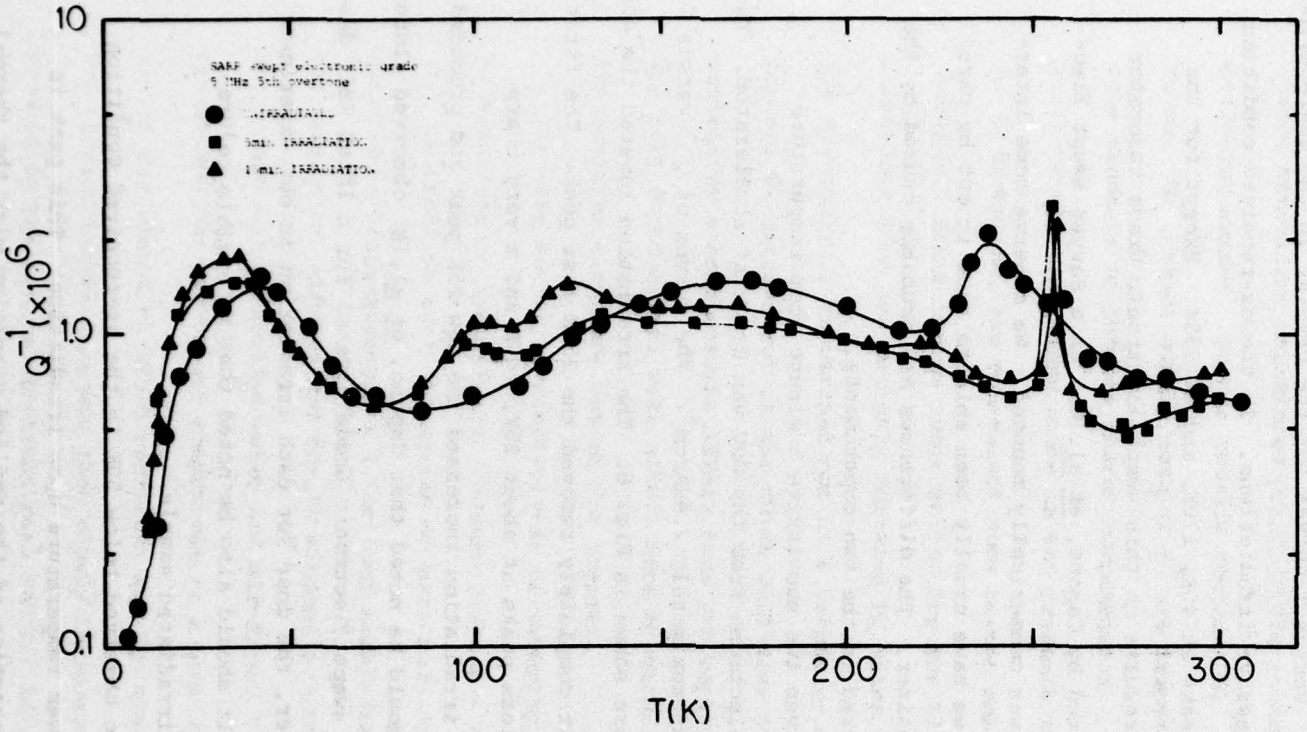

FIGURE 6. The acoustic loss, Q^{-1}, is shown for a SARP swept electronic grade resonator. Irradiation shifts the low temperature loss, introduces new loss peaks at 100 and 125 K. The 240 K loss peak is removed by the irradiation.

synthetic quartz. The acoustic loss can be related to the relaxation time of the thermal phonons (2) which can be determined from low temperature thermal conductivity measurements. The increase in acoustic loss upon irradiation at this low temperature would be reflected in an increased thermal conductivity. Berman (10) has reported that the low temperature thermal conductivity of a synthetic quartz sample increased upon irradiation. We do not see the 50K loss peak that is attributed to Na^+ impurity ions. The loss peaks at 100K and 125K in the irradiated material probably correspond to the 100K and 130K peaks listed in Fraser (1) as being due to the Al^{3+}-hole center. The very broad loss peak centered at 170K which decreases slightly upon irradiation does not seem to correlate with the mechanisms given in Fraser's review paper.

The loss peak at 235K falls near the temperature range where loss due to OH modes have been observed. Our infrared absorption results suggest that there are several different possible H^+ sites available in the crystal and that irradiation can alter their relative population. After the irradiation, the 235K loss peak is replaced by a very sharp peak at 257K. Perhaps, the irradiation has caused only one type of site to be populated.

E. Summary and Future Work

Most of this reporting period has been spent developing and testing the acoustic loss measurement system. It is now in good working order. Our initial measurements of the Q^{-1} versus T for the swept Electronic Grade resonator shows several interesting changes when the sample is irradiated. Since this material is not as well characterized, we plan to carry out most of our measurements on Sawyer Premium Q material. Isochronal annealing studies and low temperature irradiation will be used to try to identify the defects responsible for the loss changes. The results will also be correlated with our ESR and optical studies.

III. ELECTROLYSIS

Electrolysis or sweeping has been shown to improve the radiation hardness of quartz oscillator crystals (8). The process can be used to remove or exchange monovalent impurities (11,12,2). The process is thought to work in the following manner. Quartz usually contains Al^{3+} ions which are in Si lattice sites. Na^{+}, other alkali ions, or H^{+} are trapped near the Al^{3+} in the large Z axis channels to provide charge compensation. If the crystal is heated to a sufficiently high temperature in the presence of an electric field applied in the Z direction, the monovalent ions become mobile and drift down the Z axis channels. Since charge compensation for the Al^{3+} must be maintained, the monovalent ions are probably replaced by holes to form Al^{3+}-hole centers if the electrolysis is carried out in a vacuum or a clean inert gas (12). If the process is carried out in air which will also contain H_2O or other hydrogen containing atmosphere, the alkali ions are replaced by H^{+}. Kats(11) and Fraser (2) have doped quartz with alkali ions by depositing the appropriate salt on the positive electrode end of the crystal.

We have set up an electrolysis or sweeping system which allows us to run in a variety of atmospheres. Figure 7 shows a block diagram of the system.

In order to test the system we have made our initial runs on Sawyer Electronic Grade quartz. A 1.5cm long sample was cut from a lumbered bar. The sample was then etched for 30 minutes at room temperature in concentrated HF, rinsed with distilled water and air-dried. It was then mounted in the system and the system was pumped out to a good diffusion pump vacuum. The sample was heated to 500°C overnight and 700 TORR of gettered Ar was introduced. The furnace temperature was then slowly increased until the thermocouple mounted in the bottom electrode read 540°C. At that time, the electric field was applied and slowly increased to 690 V/cm. The initial sample current density was approximately $2\mu A/cm^2$. Figure 8 shows the current density versus time for

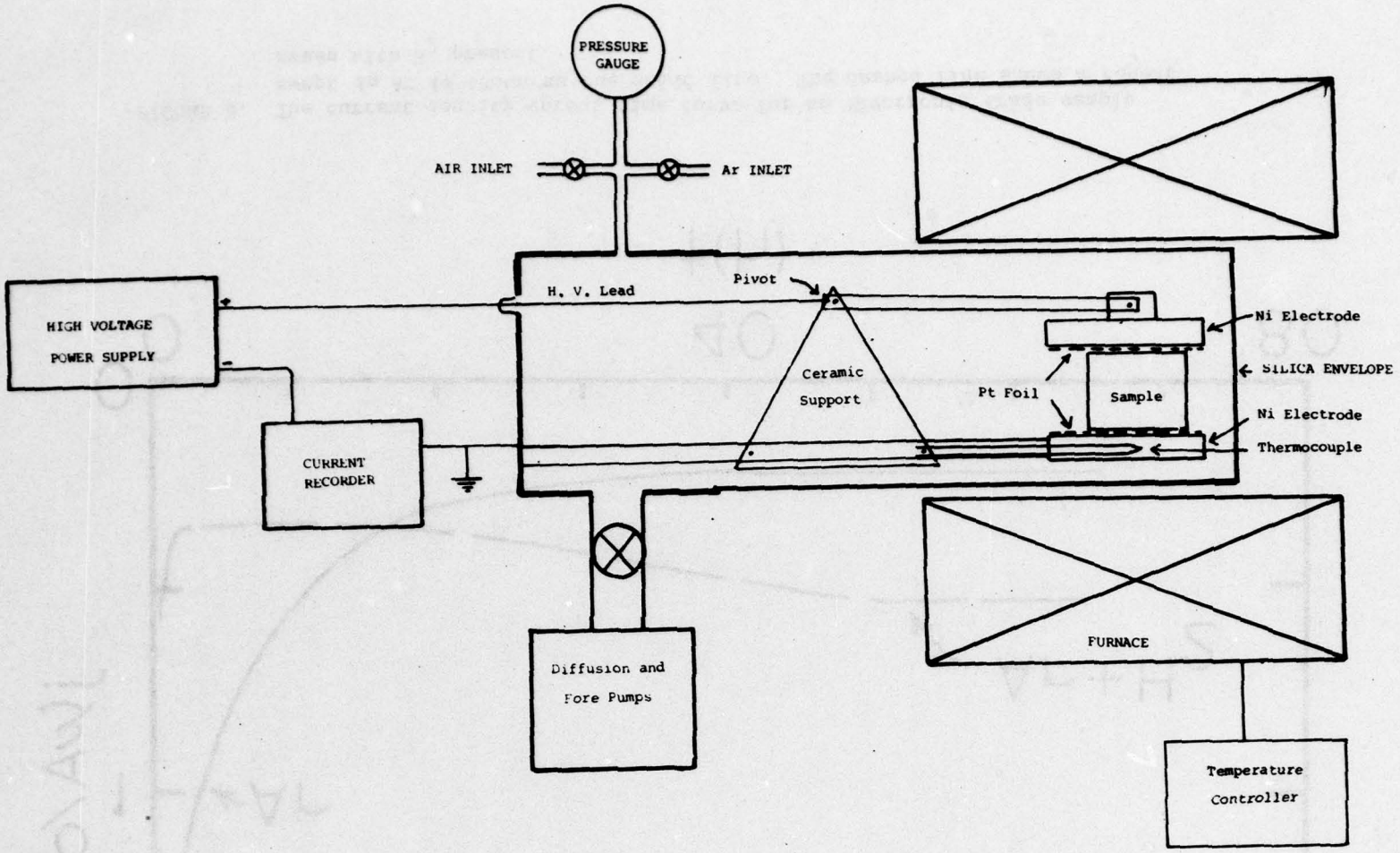

FIGURE 7. The electrolysis system.

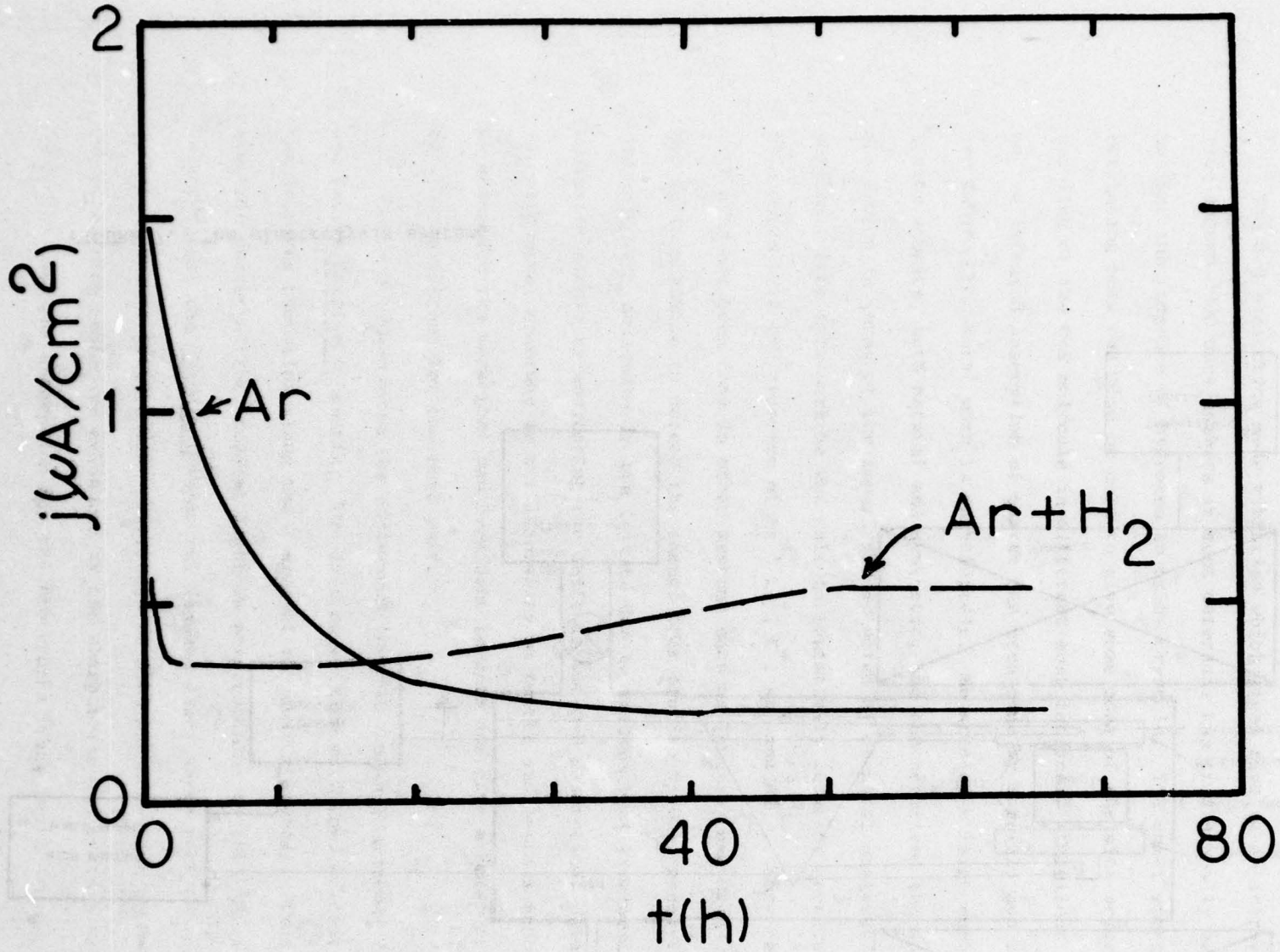

FIGURE 8. The current density versus time curve for an Electronic Grade sample swept in Ar is shown as the solid line. The dashed line shows a repeat sweep with H_2 present.

this run. The sample current decreased for several days and then remained constant. After the current had been constant for two days the sample was slowly cooled to room temperature with the electric field applied. Although a complete analysis of this test run is not complete the current density versus time behavior is consistent with the picture of sweeping out alkali ions. Persumably, they are replaced with holes since the run was made in a hydrogen free atmosphere. The ir spectrum of this sample is discussed in the next section of the report. A second run was made on the same sample using the same procedure except that about 10 TORR of H_2 was mixed with the Ar. In this case, after an initial drop, the current density showed a slow increase with time. If the hole picture described above holds, then this run has possibly replaced the holes with H^+ ions. Further studies are being carried out on Sawyer Premium Q material.

IV. INFRARED STUDIES

The O-H stretching mode vibration which gives rise to an infrared absorption around 3300 wave numbers in most materials has traditionally been used to monitor the presence of hydrogen in oxide crystals. The exact energy of this stretching mode can also be used to give some idea of the site symmetry or the coupling of the O-H molecule in different host lattices. Excellent research on the infrared absorption of quartz has been done by Kats(11) and by Brown and Kahan (13). Kats' work is encyclopedic. He studied a large number of quartz samples, both natural and synthetic, and characterized the infrared absorption in terms of the impurities detected by chemical analyses of the samples. From this work he was able to tentatively identify certain absorption peaks with the presence of Na^+, Li^+, K^+, Ag^+ and Al^{3+}. More recently work also has been done in other systems such as TiO_2(14) and MgO (15). In MgO it is possible to detect the change from brucite $Mg(OH)_2$ precipitates to isolated $Mg(OH)_2$ molecules in the lattice due to various heat treatment or due to radiation simply by monitoring the shift in the O-H absorption. Similar work is, of course, underway in our laboratory on quartz and in this annual report we summarize the work that has been done to date and give a brief projection of what is planned for the next year.

Figure 9 illustrates the difference between Sawyer Electronic Grade quartz and Sawyer Premium Q quartz. The data were taken with the incident beam of the infrared radiation along the Z axis of the quartz crystal. Thus the electric vector of the incident light is perpendicular to the Z-axis. It can be noted that the Premium Q spectrum (dashed line) shows rather broad intrinsic quartz lattice mode absorption at 3200 and 3300 wave numbers. The O-H stretching modes are evidenced by the sharp peaks and exhibit much less intensity than the absorption for the Electronic Grade (solid line). In fact,

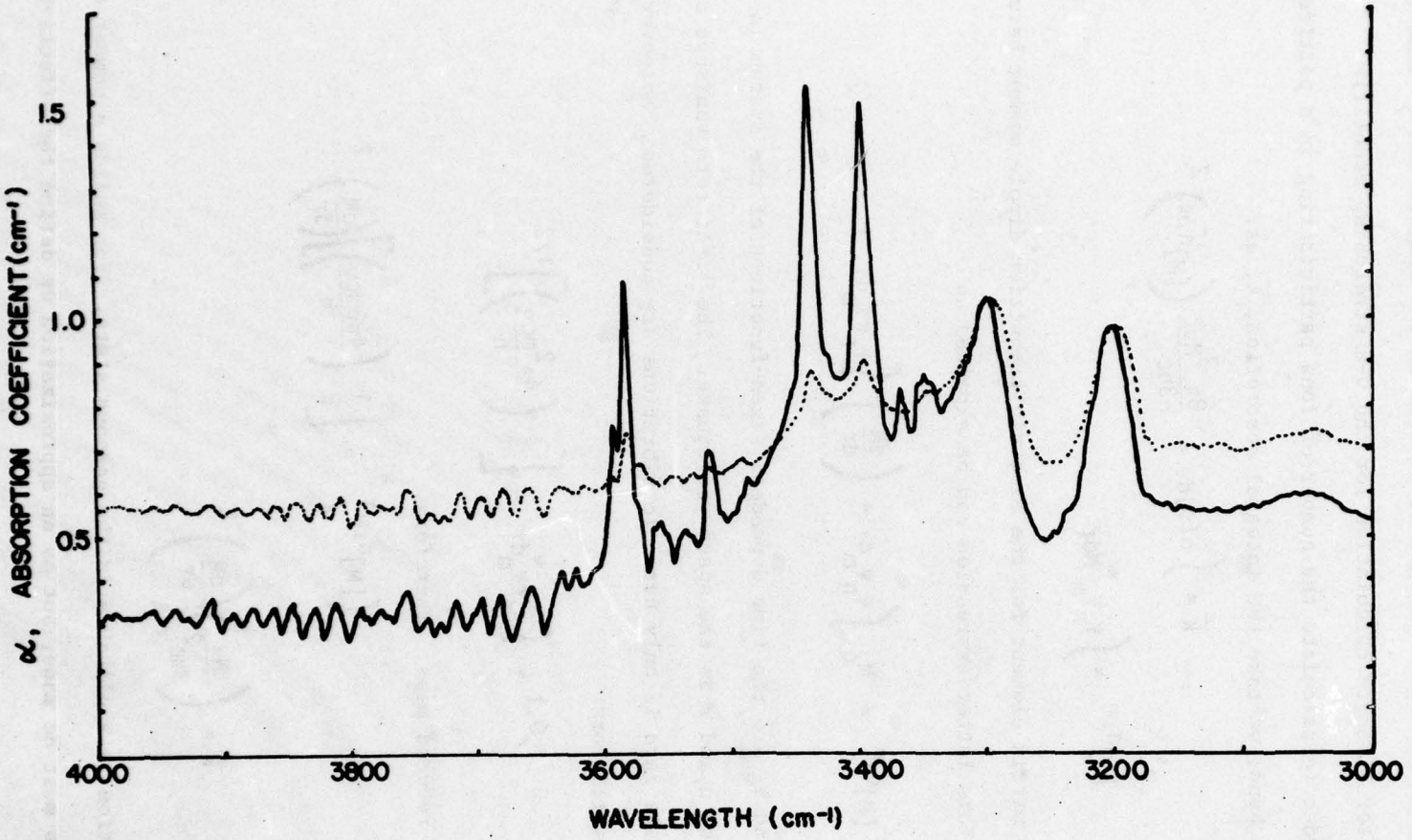

FIGURE 9. I.R. absorption spectra of Z cut samples of Sawyer Electronic Grade (solid line) and Premium Q (dashed line) quartz. The spectra were run at approximately 90 K.

an estimate of how much hydrogen is present in the samples can be made from an oscillator strength calculation for the O-H stretching mode(11).

In order to calculate the number of ions participating in a particular absorption band, we take the integral absorption, $\bar{k}$, as:

$$\bar{k} = \int \alpha(\nu) d\nu = \frac{8\pi^3 N\nu}{3hc} \left([M]^{n,m}\right)^2$$

where

$$[M]^{n,m} = \int \psi_n \psi_m^* M d\tau$$

and is the matrix element for the electric transition dipole moment between states m and n. This latter expression can be expanded as

$$[M]^{n,m} = M_o \int \psi_n \psi_m d\tau + \left(\frac{dM}{dr}\right) \int \psi_n r \psi_m d\tau + \ldots$$

where ψ_n and ψ_m are the time dependent eigen-functions of the system in the two states m and n, and r is the space coordinate. The first term vanishes and the third term is zero if only harmonic vibrations are considered. Moreover, for harmonic oscillators

$$r^{0,1} = \int \psi_n r \psi_m^* d\tau = \left[\frac{1}{2}\left(\frac{4\pi^2 mc\nu}{h}\right)\right]^{1/2}$$

with m the reduced mass. Therefore,

$$\left([M]^{n,m}\right)^2 = \left[\frac{1}{2}\left(\frac{4\pi 3mc\nu}{h}\right)\right]\left(\frac{dM}{dr}\right)^2$$

and

$$\bar{k} = \left(\frac{N\pi}{3mc^2}\right)\left(\frac{dM}{dr}\right)^2 .$$

This equation is applicable in the gaseous state. For solids a number of corrections must be made, but as an approximation we define the effective

charge p by $e = pe_o = \frac{dM}{dr}$ where e_o = electron charge.

Thus for 3 degrees of freedom we find

$$\bar{k} = \frac{N_H e_o^2 p^2 \pi}{3mc^2} .$$

For polarized light this reduces to

$$\frac{N_H e_o^2 p^2 \pi}{mc^2} .$$

If the absorption bands are Gaussian, they can be described by the relation

$$\alpha(\nu) = \alpha_{max} \exp \left\{ - (4 \ln 2/H^2) h^2 \nu^2 \right\}$$

where α_{max} is the maximum absorption coefficient and H is the band width at half maximum. Then,

$$\bar{k} = \int \alpha(\nu) d\nu = \left\{ \frac{\pi^{1/2}}{2(\ln 2)^{1/2}} \right\} H\alpha_{max} = 1.0645\ H\alpha_{max}$$

and

$$N_H = \frac{\bar{k}\, mc^2}{\pi e_o^2 p^2} = H\alpha_{max} \left(\frac{mc^2}{\pi^{1/2}\, 2(\ln 2)^{1/2} e_o^2 p^2} \right) .$$

For light propagating along the Z axis of the crystal the electric vector of the incident light is perpendicular to Z, $E \perp Z$, and

$$N_H = \frac{4.003 \times 10^{15}}{p^2}\ H\alpha_{max} .$$

The values of p vary from 0.43 to 0.52.[11]

Bates and Perkins(14) working with TiO_2 have also found a similar relationship for the O-H stretching mode and have determined that $N_H = 1.8 \times 10^{16} H\alpha_{max}$. This is in good agreement with the work shown above for effective charge of $p = 0.5$. From this type of calculation we can now estimate the hydrogen content in both the Premium Q and Electronic Grade Sawyer quartz shown in Fig. 9. Integrating the areas in all the absorption bands in both samples we find that for Premium Q there are approximately 10^{17} hydrogens/cm^3 whereas in the Electronic Grade material there are approximately 8×10^{17} hydrogens/cm^3. An interesting question that must be answered is, "What is the charge compensator for the hydrogen which is in the quartz lattice?". Traditionally Al or B which are incorporated in quartz as 3^+ ions substituting for Si^{4+} have been taken to be the charge compensators. Kats' work illustrates very graphically that the amount of Al and Fe present in his samples correlated directly with the hydrogen or deuterium concentrations. We have had mass spectroscopy done at the Oak Ridge National Laboratory on several of our samples. This same correlation appears valid in our samples although the results are only preliminary at this time.

Once the hydrogen is incorporated into the lattice through the growth process it would be very informative if it were possible to shift the hydrogen from one site to another by either radiation treatment, heat treatment or sweeping. Figure 10 illustrates the effect of 300 K 1.5 MeV electron irradiation on Sawyer Electronic Grade quartz, cut in such a way that the light propagates along the Z-axis of the crystal. Notice that some of the bands decrease. The two intrinsic quartz lattice mode bands at 3200 and 3300 cm^{-1} remain constant and act as normalization points. Two new bands grow in - one at 3306 and the other at 3367 cm^{-1}. These bands have, of course, been observed much earlier by Kats, Brown and Kahan, and others. They have been identified

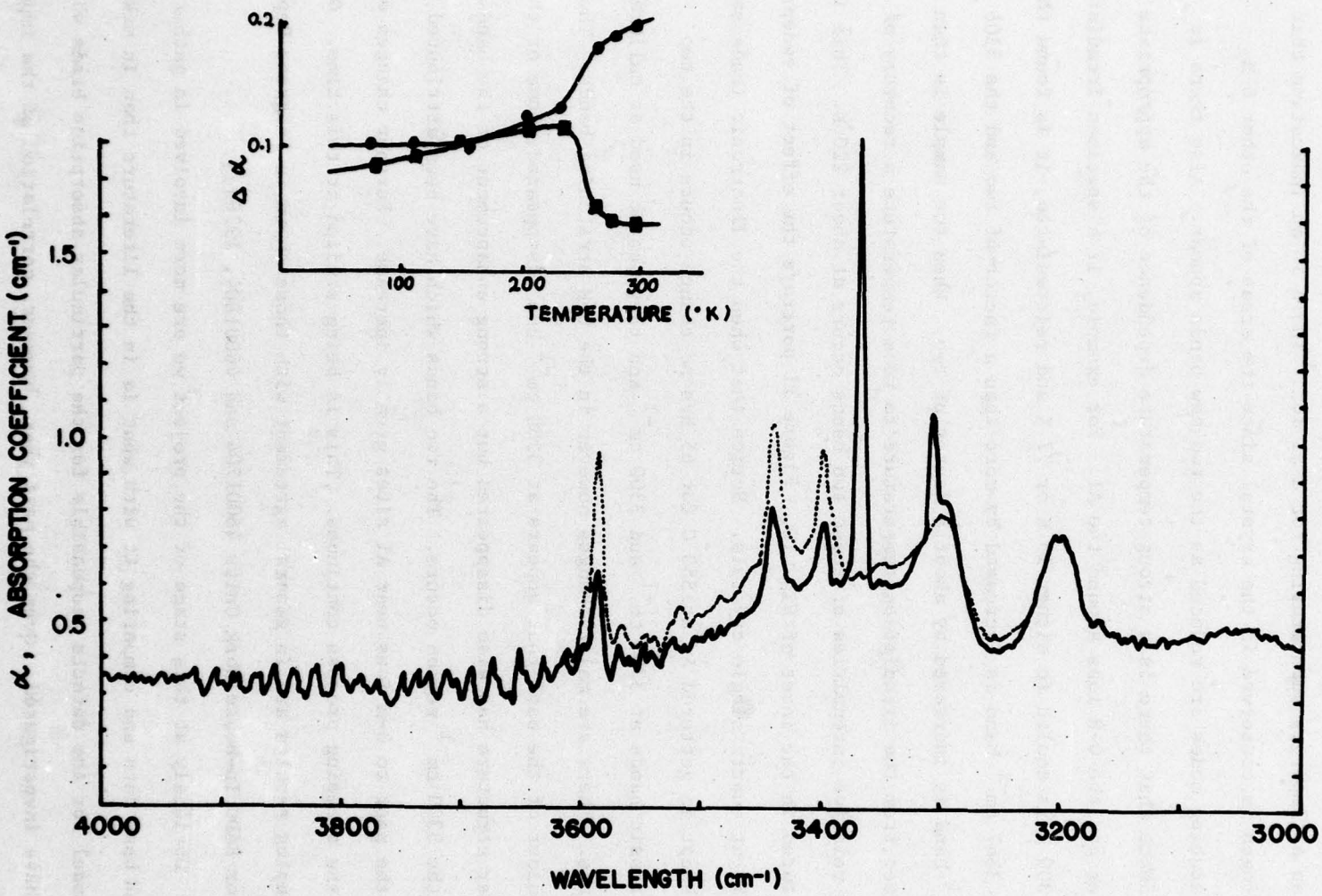

FIGURE 10. I.R. absorption spectra of Sawyer Electronic Grade quartz, as received (dashed line) and after a room temperature electron irradiation (solid line).
Inset: annealing characteristics of the 3367 cm^{-1} (circles) and 3306 cm^{-1} (squares) absorption bands, after a room temperature electron irradiation followed by a low temperature irradiation.

as due to O-H ions in the presence of Al i.e., an O-H bond in the vicinity of an Al impurity substituting for a Si ion. There is an indication that hydrogen is conserved in the crystal since the areas of the other O-H stretching modes are reduced as the two new bands appear. Also there is evidence that there is a strong temperature dependence of the appropriate sites for the O-H ions around the Al. For example, if a specimen irradiated at 300 K is cooled to either 15 K or 77 K and reirradiated, it is found that the 3367 cm^{-1} band is decreased by more than a factor of two and the 3306 cm^{-1} band is increased by about a factor of two. When the sample is then warmed from the irradiation temperature to room temperature a recovery of the relative intensities of these two bands occurs at about 220 K. This is pictured in the inset of Fig. 10. Figure 11 portrays the effect of sweeping on Z cut quartz single crystals. Notice that when the Electronic Grade sample is swept in gettered Ar at 550 C for 65 hrs no change occurs in the two intrinsic bands at 3200 cm^{-1} and 3300 cm^{-1} and they can be used as calibration points. There are major changes however in the O-H stretching bands. The shoulder of the band that appears at 3580 cm^{-1} has disappeared, some of the other structure has also disappeared but a strong enhancement of the bands in the 3300 cm^{-1} region occurs. The two bands which have been attributed in the past to O-H ions near Al sites greatly increase. Further changes occur as the sweeping process continues. This is being studied at this time. Our sweeping results are in general agreement with those shown in Progress Report 8 for RADC In-House Work Units 46001704 and 46001804, 1978(1).

Obviously at this stage of the project we are more involved in gathering good base data and comparing it with what is in the literature than in making a model for the defects responsible for the particular absorption bands which we have investigated. Over the next year, however, correlation of the impurity

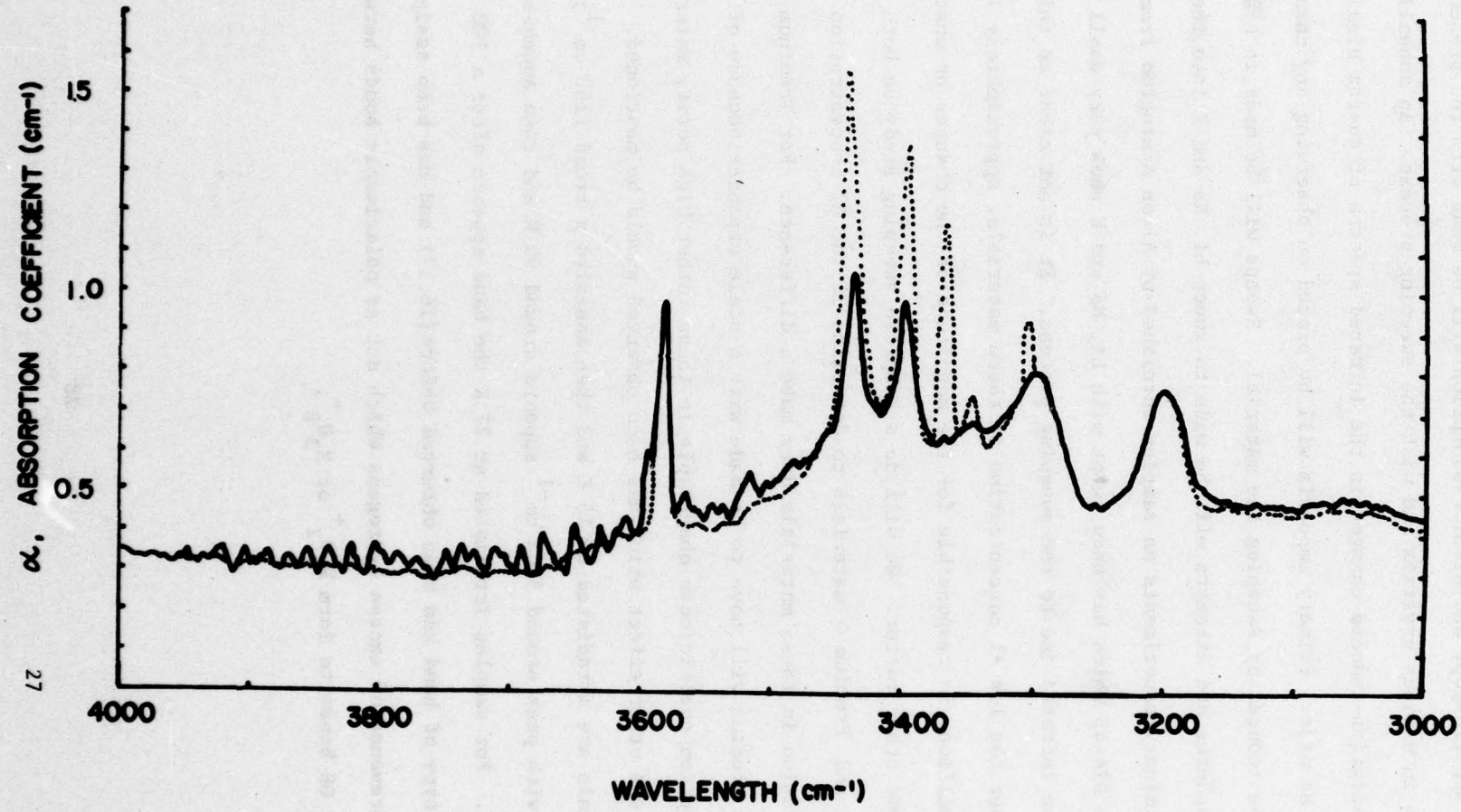

FIGURE 11. I. R. absorption spectra of Sawyer Electronic Grade quartz, as received (solid line) and after sweeping for 65 hrs at 550°C in a gettered Ar atmosphere (dashed line).

analyses from Oak Ridge National Laboratory which are being done by both mass spectroscopy and atomic absorption will be made with the presence of bands in various crystals and with the sweeping process. An annealing study of radiation-induced changes in the infrared spectra of quartz single crystals will be made. Primary emphasis will be placed on observing any changes that can be induced by sweeping the material. Sweeps will be made in hydrogen atomspheres and attempts will be made to sweep Li, Na and K into the samples. Preliminary experiments on samples furnished by Alton Armington from SARP boule D14-45 which has been swept with Li, Na and K show very small changes in the infrared due to the sweeping process. It is not clear at this time whether the low Al concentration in these materials, approximately 10 parts per million, is responsible for the magnitude of the changes or whether it is some other factor. We will do a complete sweeping study on both Electronic Grade and Premium Q materials to determine if the Al concentration or B concentration in these materials does make a difference. For Preminum Q samples these studies will have to be made with a scale expander because of the small absorption coefficients observable in these rather high purity materials.

One other effect which has been observed should be mentioned. When SiO_2 crystals are irradiated at 15 K and then annealed a broad (150 cm^{-1}) infrared band with peak around 3300 cm^{-1} appears around 60 K and then anneals around 160 K. For samples irradiated at 77 K the band appears after a 100 K anneal. This type of band has been observed before (16,17) and has been assigned to the presence of excess hydrogens which act as polarizable bonds between other OH bonds to form $H_5O_2^+$ or $H_3O_2^-$.

V. MAGNETIC RESONANCE

A. Thermal Stability Studies

During the past year, we have investigated three classes of paramagnetic defects which are produced in quartz by ionizing radiation. Trapped hole(18), trapped electron(19-21), and hydrogen atom(22) centers comprise the three classes. The experimental conditions necessary for formation and detection of each type of defect are quite different; trapped hole centers and hydrogen atoms can be observed only near liquid nitrogen temperature while trapped electron centers are observed best at room temperature.

The only trapped hole center observed thus far is associated with aluminum. The currently accepted model for the aluminum-hole center involves an aluminum ion (Al^{3+}) substituting for a silicon, with a hole trapped in a p orbital on one of the four nearest neighbor oxygen ions. Figure 12 is a schematic representation of a part of the quartz lattice showing the distorted Si-O tetrahedron. It can be seen that the four oxygen ions (open circles) do not occupy exactly equivalent sites with respect to the silicon site (shaded circle). Thus, the two oxygen ions (labeled 3 and 4 in Fig. 12 closest to the Al^{3+} ion will be preferred as hosts for the trapped hole. However, the difference in trap depth between the two pairs of oxygen ions is small enough (approximately 0.03 eV) that at room temperature there is a very rapid jumping of the hole among the four oxygens surrounding the aluminum. This jump frequency is in the MHz range at room temperature and suggests that strong couplings to the acoustic vibration modes of the quartz crystal may occur. Therefore, the aluminum-hole ($Al\text{-}h^{+}$) center, possibly modified by the presence of other neighboring impurities, must be of primary interest in any investigation of the effects of radiation on quartz oscillators.

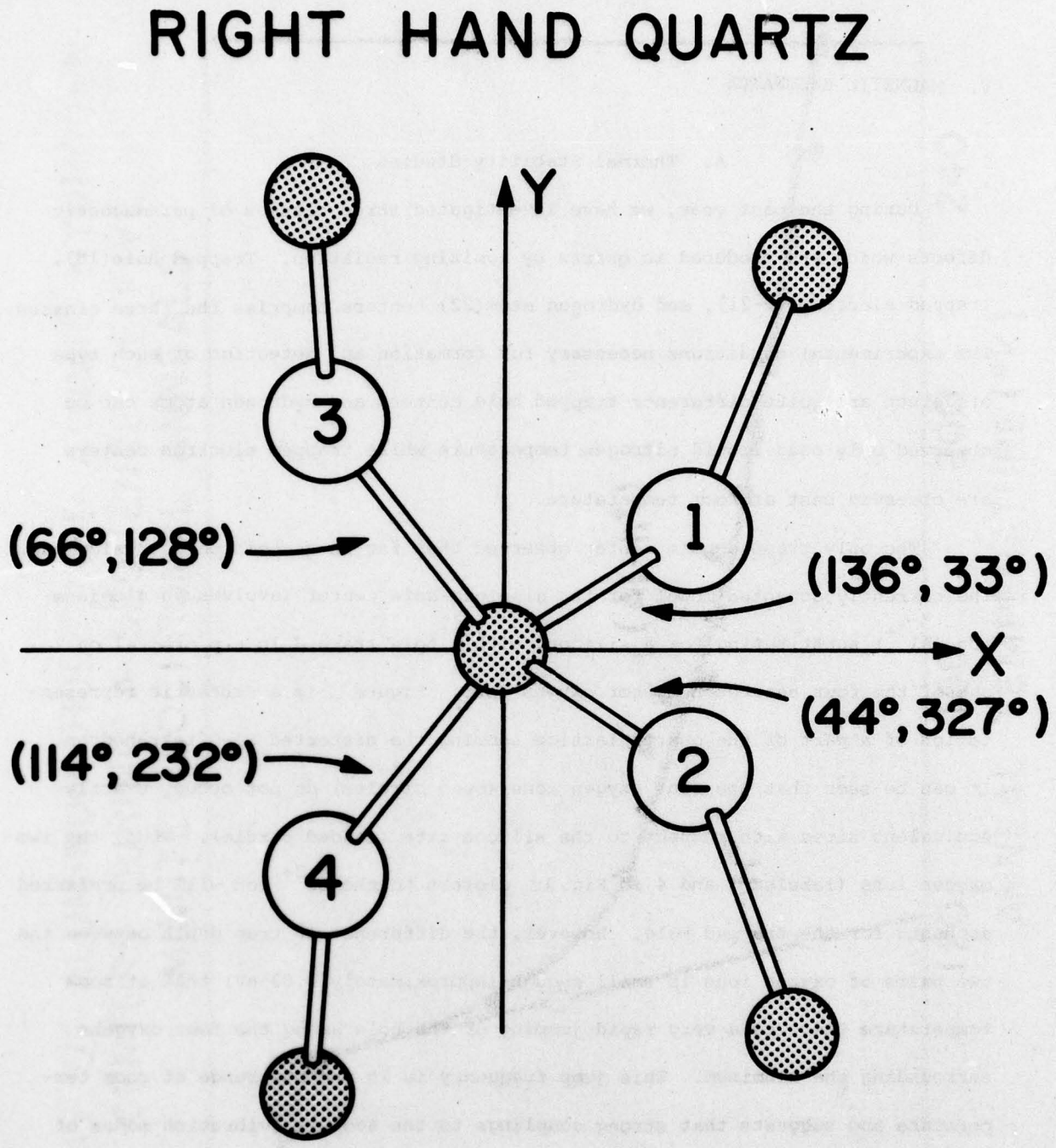

Figure 12. Structure of distorted Si-O tetrahedron.

The thermal stability of the Al-h^+ centers is illustrated in Fig. 13 for a Sawyer Electronic Grade (Z growth) sample irradiated at 77 K. Also shown in this figure is the thermal decay of the hydrogen atom. The c-axis ESR spectrum of the atomic hydrogen center contains two narrow, widely separated lines and according to the results of Weeks and Abraham(22) and Perlson and Weil(23), the atom is in an interstitial site along the open c-axis channel. The atomic hydrogen signal disappears after the 130 K anneal and at this stage the aluminum-hole center concentration has fallen to about one half its original value.

A possible mechanism for this decay of both centers near 110 K might be thermally induced mobility of the proton which then interacts with the aluminum center. However, an aluminum-hydrogen-hole complex has previously been identified(24) and its presence is not detected in our samples. Therefore, we believe that the atomic hydrogen center decays by release of its electron which then moves through the crystal via the conduction band until it recombines with the hole, thus destroying the aluminum-hole center. This process is supported by the observation of Dr. E. E. Kohnke at Oklahoma State University of a significant thermoluminescence glow peak at approximately 110 K.

Above 130 K there is a steady decrease in the aluminum-hole center concentration as shown in Fig.13 with no features that are sufficiently prominent to warrant identification as separate annealing stages. One should note that several different forms of the aluminum-hole center have been reported, notably by Mackey(24,25), in which the center is perturbed by a monovalent ion such as Li^+ or Na^+ and these anneal out between 77 K and 300 K. Also, several thermoluminescence peaks have been observed in this range, of which one at 219 K appears to result from hole release. Thus, there are a number of different processes occuring in this temperature range which result in effective charge transfer. However, we did not observe any obvious change in the shape of the

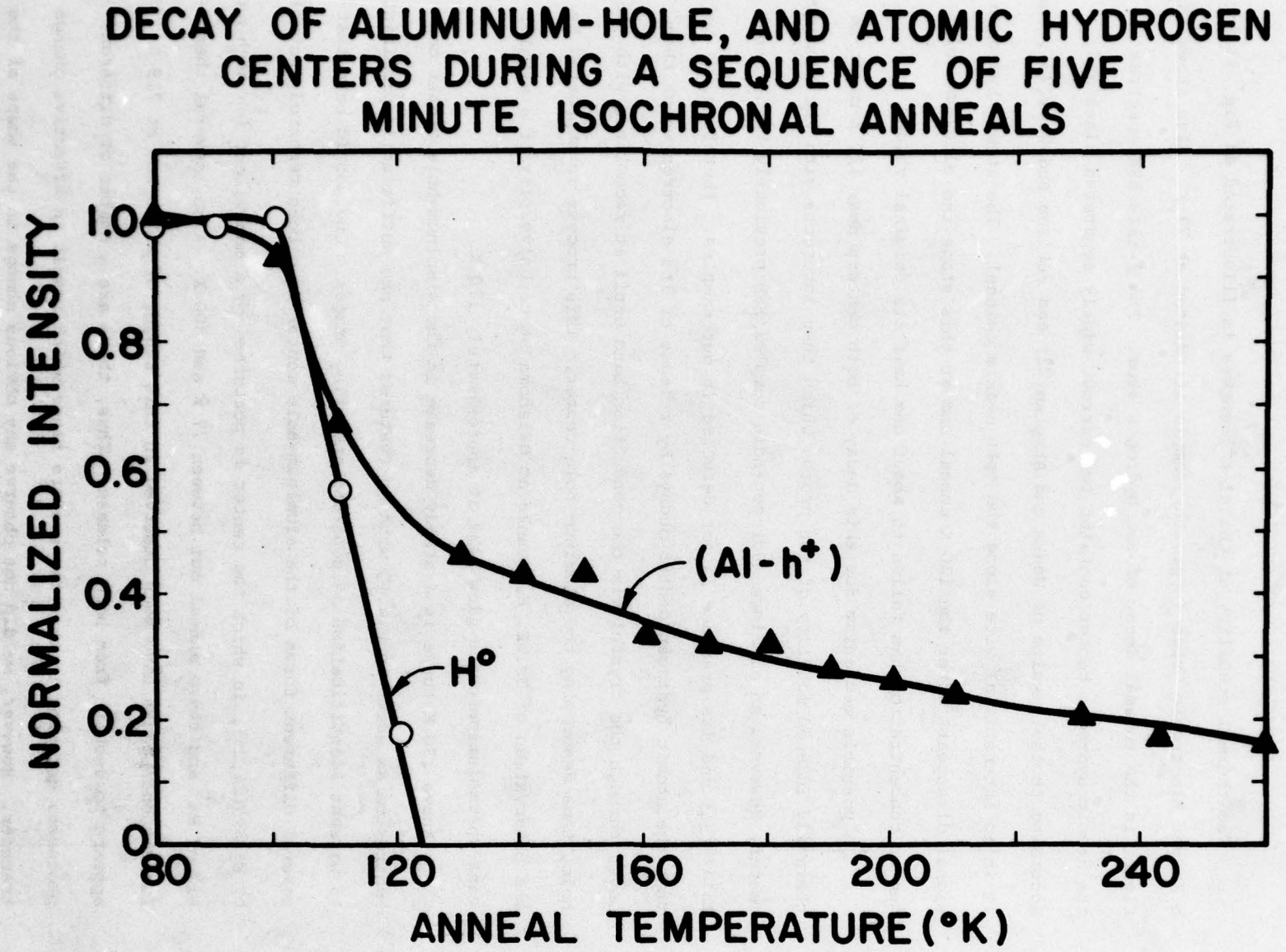

FIGURE 13. Thermal annealing results obtained by monitoring ESR spectra produced by 77 K irradiation.

ESR spectrum and so at this stage in the investigation we cannot assign any particular process to possible annealing stages.

It can be seen that by room temperature the aluminum-hole concentration has fallen to approximately 1/10 its initial value. However, a quartz sample irradiated at room temperature and examined at 77 K contained the same concentration of aluminum-hole centers as a sample both irradiated and examined at 77 K. More surprisingly, a two minute room temperature irradiation followed by a two minute liquid nitrogen irradiation produces an order of magnitude more aluminum-hole centers than when the total irradiation is given at liquid nitrogen temperature, but the annealing curves are substantially the same.

The thermal stability of the trapped hole and trapped electron centers was investigated in the region above room temperature. Figure 14 shows the annealing behavior of the E_2', E_4', and aluminum-hole centers in a Sawyer Electronic Grade (Z growth) sample irradiated at room temperature. The E_2' and E_4' centers, both of which involve a proton, anneal out at approximately 410 K. The aluminum-hole center concentration decreases steadily from room temperature, with a steeper decrease around 440 K and 525 K. Again several thermoluminescence peaks have been observed in this temperature range but no individual features on the annealing curve can be correlated with them. The relatively small effect of the annealing out of the E_2' and E_4' centers on the aluminum-hole center concentration points to there being significantly fewer E' centers than Aℓ centers.

The sample from which the previous results were taken showed only a very small E_1' signal which was observed after the 550 K anneal. Earlier, probably less pure, samples we examined did show a considerable E_1' center signal as illustrated in Fig. 15. The E_1' signal is observed to grow in slowly as the aluminum center anneals out reaching a maximum concentration at about 560 K and annealing out near 600 K. The E_2' and E_4' centers were observed as before but for clarity are not shown in Fig. 15.

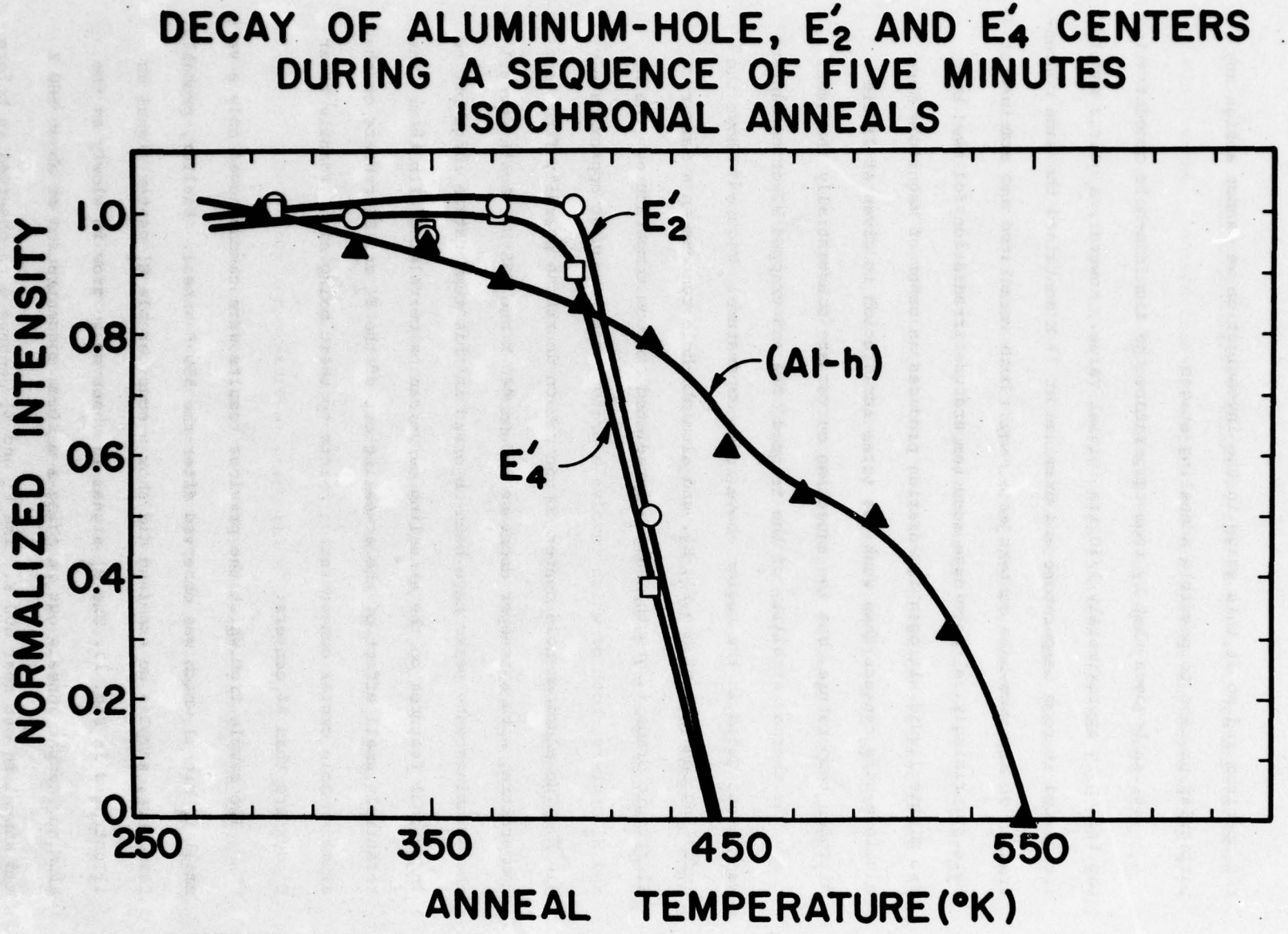

FIGURE 14. Thermal annealing results obtained by monitoring ESR spectra produced by 300 K irradiation.

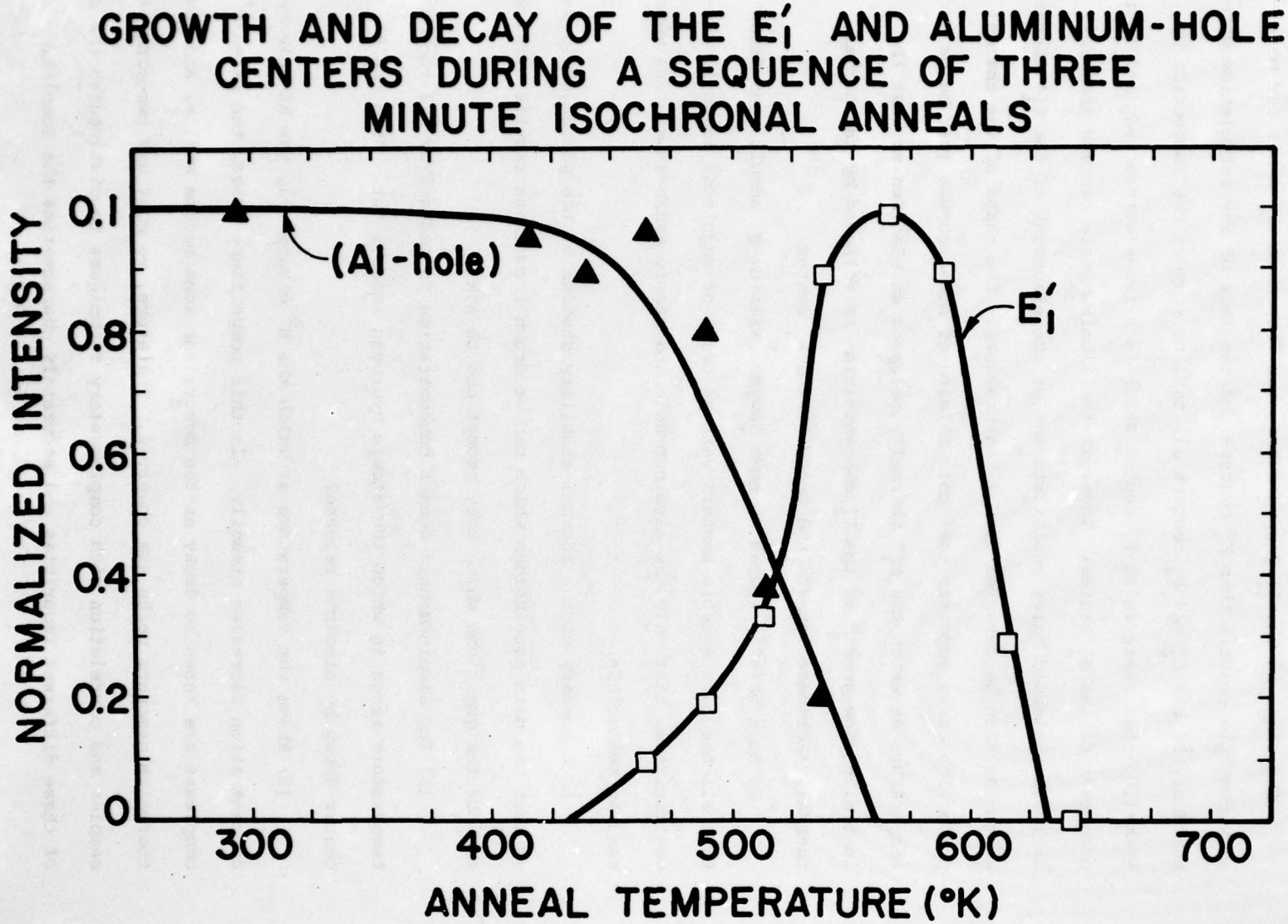

FIGURE 15. Thermal annealing results showing the growth and subsequent decay of the E_1 center.

The shape of the E_1' growth curve, the fact that there are far more aluminum-hole centers than E_1' centers and the lack of any correlation with the decay of the E_2' and E_4' centers all tend to support the suggestion by Weeks (20) that there is an E_1'' center which is a two-electron trap and is the precursor of the E_1' center. Thus, as the aluminum-hole centers thermally decay the released holes annihilate one of the electrons of the E_1'' center which can then be detected by ESR measurements. The shape of the thermal production curve suggests that this release of holes occurs just below the temperature at which the E_1'' thermally releases an electron so that the initially slow growth of the E_1' concentration is followed by the normal, thermally-activated growth and decay of the E_1' center.

We have briefly looked at some Sawyer Premium Q samples and found that all the paramagnetic centers were an order of magnitude lower in concentration so that only the aluminum-hole and atomic hydrogen centers were readily measurable.

As a summary of the thermal stability studies of the paramagnetic defects, we list the main conclusions which can be drawn from these results along with some of the questions which they prompt one to ask.

(1) The aluminum-hole center concentration is reduced by 1/2 in the temperature range in which the atomic hydrogen anneals out. Does the H^o center decay by electron release?

(2) Above the temperature at which the H^o disappears, the Aℓ-hole center concentration decreases steadily. In this temperature range, the $[Aℓ\text{-}h/M^+]$ complexes are known to decay as the monovalent ions become mobile, and several thermoluminescence peaks are observed. Therefore, we must use sweeping of samples and correlation with complementary techniques to distinguish the effects of these different impurities and accurately characterize the samples.

(3) Irradiation at 300 K followed by irradiation at 77 K produces an order of magnitude more centers than irradiation at 77 K or at 300 K alone. What significance does this have in relation to (2) and to data from infrared and optical absorption studies?

(4) The E_2' and E_4' centers decay at the same temperature. Are these just two forms of the same basic center despite conflicting evidence from ESR studies of the centers individually?

(5) The growth of the E_1' center (if seen) coincides with the annealing of the Aℓ-hole centers, not with the disappearance of the E_2' and E_4' centers. Does thermal release of holes transform the precursor double electron trap (E_1'') to the E_1' center?

(6) The number of hole traps appears to be far greater than the number of electron traps. Is there a "reservoir" of so-far undetected electron traps compensating for the large hole-trap concentration?

B. Structure of the E_4' Center

In addition to the investigation of the annealing characteristics of the various centers, a more detailed study of one center, the E_4' center, was undertaken. As will be seen, both the E_2' and E_4' centers are associated with hydrogen and thus are of considerable importance in developing an understanding of the interstitial cation mobility (radiation-induced as well as thermally-induced) and the general radiation response of quartz.

Figure 16 shows the ESR spectra of the E_2' and E_4' centers taken at room temperature with the magnetic field parallel to the z axis. The thermal stability investigation described in the preceding section showed that these two centers have nearly identical annealing characteristics. The E_2' center spectrum contains a pair of lines as a result of a weak hyperfine interaction with a nearby proton. The E_4' center spectrum contains sets of four lines.

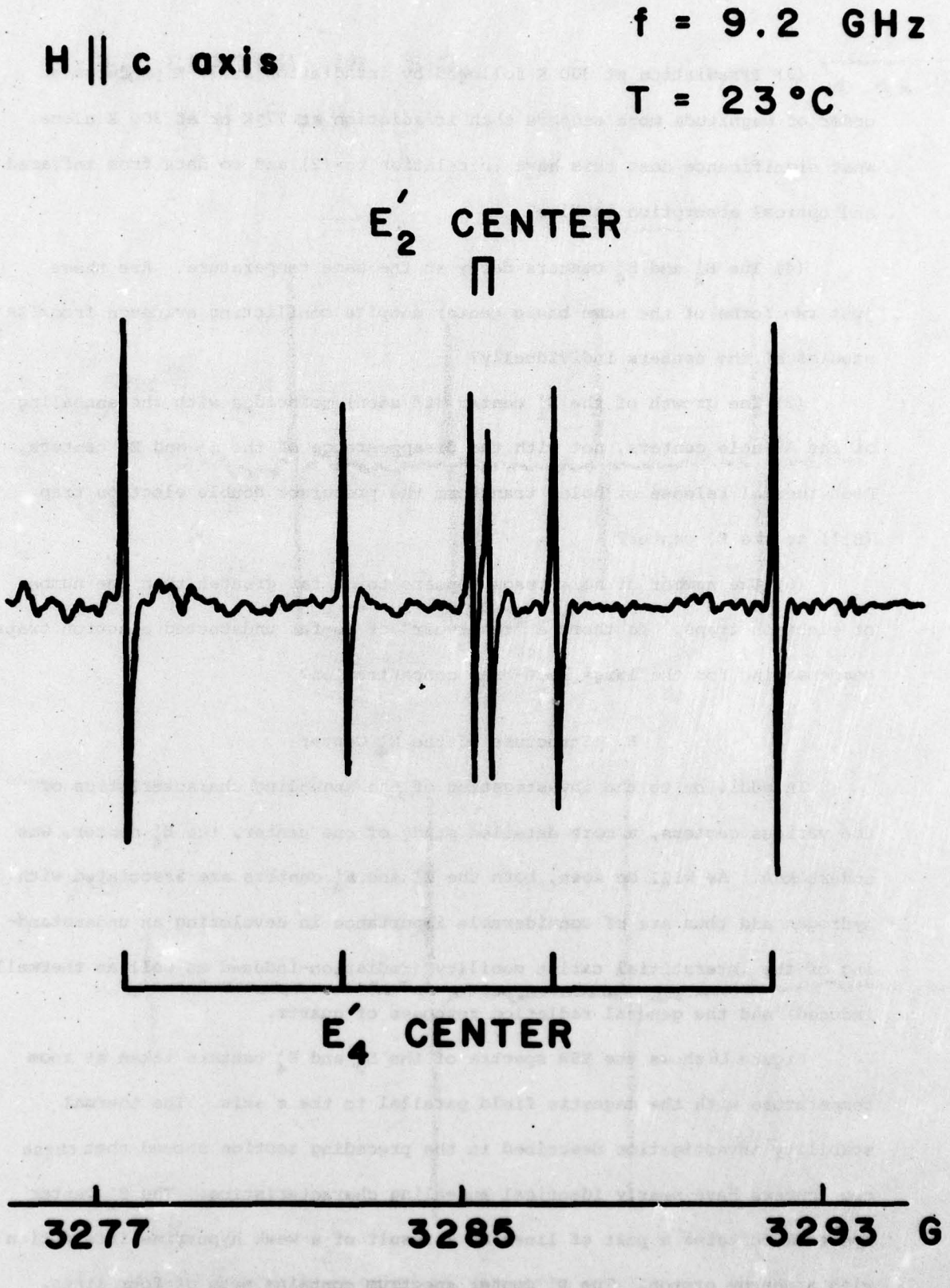

FIGURE 16. ESR spectra of E_2' and E_4' centers.

For both centers, the ESR spectrum is simplest when the magnetic field is oriented parallel to the z axis as in Fig. 16.

The ESR spectrum of the E_4' center is shown in Fig. 17, the upper trace was taken at a microwave frequency of 9.2 GHz and the lower trace was taken at 20.1 GHz. E_2' centers were also present in the sample but their lines have been eliminated from Fig.[17] so that emphasis can be placed on the E_4' center. One can clearly see that the relative intensities of the inner and outer pairs of lines for the E_4' center are substantially altered by the change in microwave frequency, and that the splitting of each pair of lines has also changed. The only way to interpret this large magnetic field dependence is to consider forbidden transitions within a spin system having S = 1/2, I = 1/2.

The spin Hamiltonian for such a spin system contains three terms; the electron Zeeman, the hyperfine, and the nuclear Zeeman. Figure 18 shows the corresponding energy level diagram when the hyperfine term and the nuclear Zeeman term are comparable in magnitude. To first order, the upper two energy levels are split by the amount $g_N\beta_N H - A/2$ where A is the hyperfine interaction. The two contributions nearly cancel making the energy separation very small and introducing considerable mixing of the basis states. The lower two energy levels are split by an amount $g_N\beta_N H + \frac{A}{2}$, which is large enough to prevent significant mixing of the basis states. The four possible transitions are indicated. The center two transitions are allowed, that is $\Delta M_I = 0$, while the outer two transitions are forbidden, $\Delta M_I = \pm 1$. At the bottom of the figure, the resulting spectrum is shown which is similar to our 20 GHZ spectrum. The center pair of allowed lines are split by A in first order and the forbidden outer pair of lines is split by $2g_N\beta_N H$. The forbidden line splitting is a direct measure of the nuclear magnetic moment.

In order to determine the g tensor and hyperfine tensor parameters, a complete angular study of the E_4' center was carried out at 20.1 GHZ. The

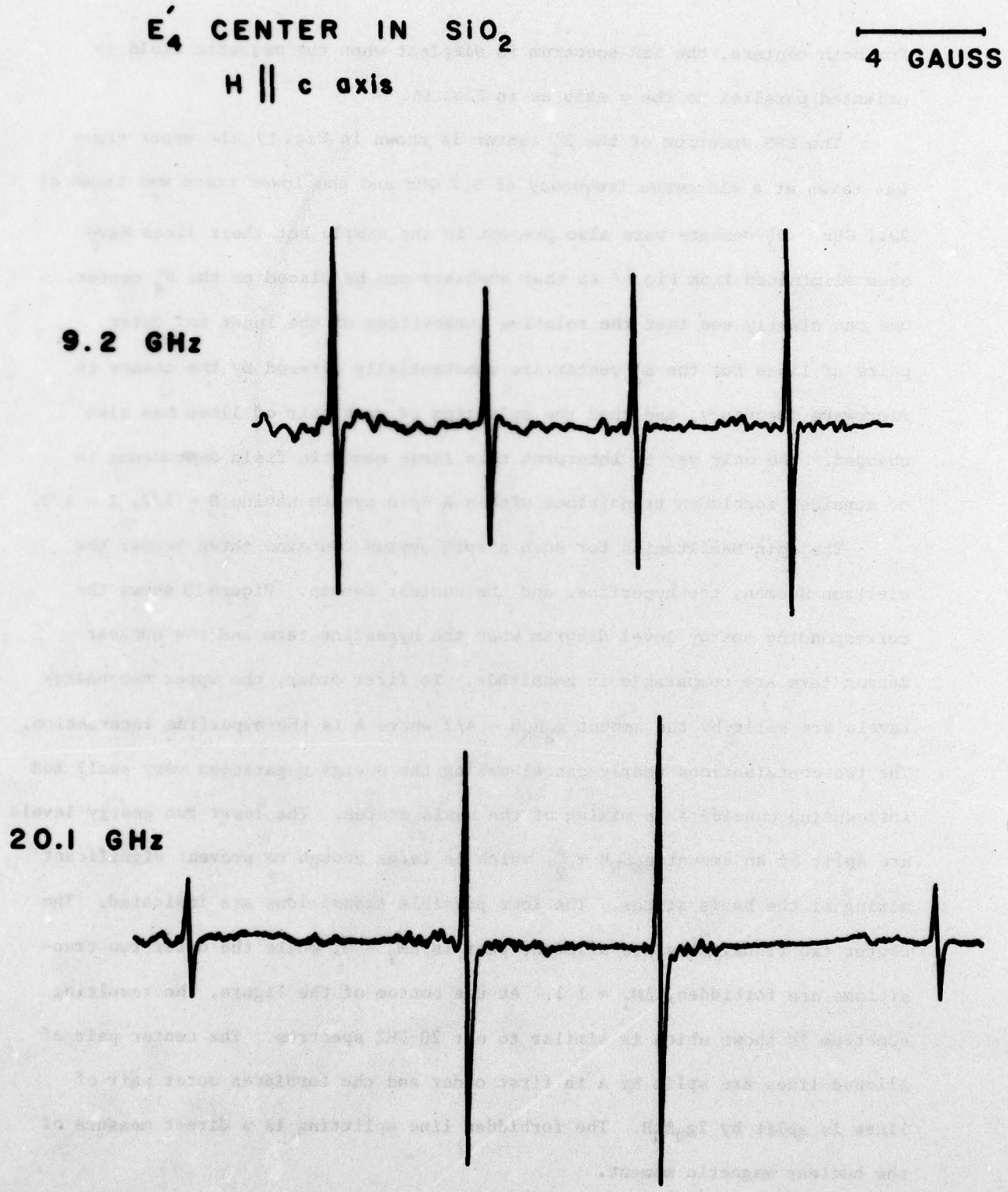

FIGURE 17. Dependence of E_4' ESR spectrum on microwave frequency.

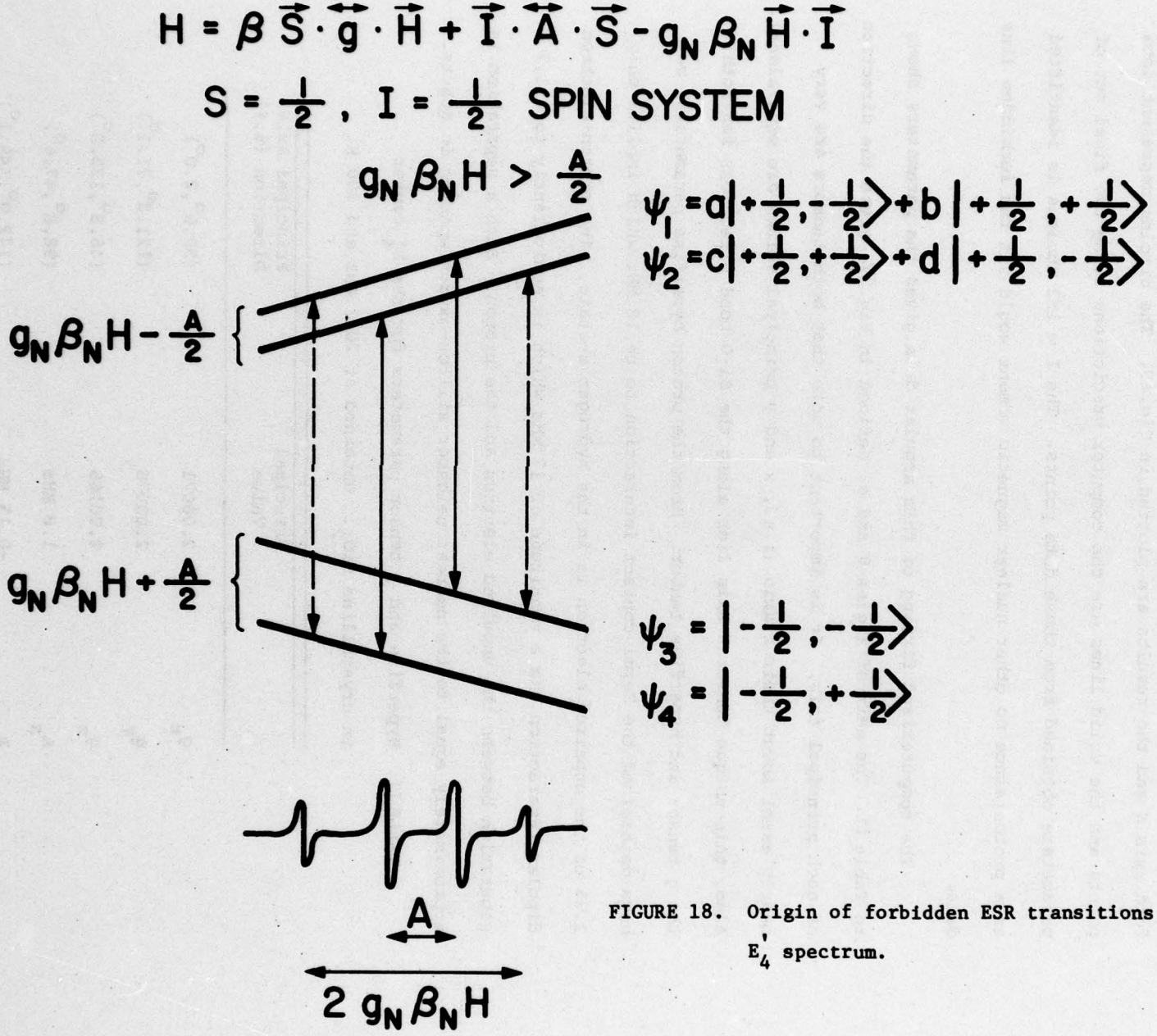

FIGURE 18. Origin of forbidden ESR transitions in the E_4' spectrum.

magnetic field was rotated from +Y to -Y in the plane perpendicular to the two-fold axis X and the results are plotted in Fig.19. The circles represent data points and the solid lines are the computer predictions using the final set of parameters obtained from these data points. The I = 1/2 nucleus is identified as a proton since no other nuclear magnetic moment would fit the forbidden line data.

The computerized fitting of this angular data gives the parameters shown in Table II. The pair of angles θ and ϕ, defined in Fig.12, gives the direction of each principal axis. It is important to note that both tensors are very nearly axial about their z axis (i.e., x and y principal values are equivalent). Also, this unique tensor z axis lies along the Si-O bond directions for both the g tensor and hyperfine tensor. From the proton hyperfine parameters, we have determined the Fermi contact interaction to be 18 MHz which implies only 1.3% of the unpaired electron is in the hydrogen s-state. The proton-electron dipolar interaction has a magnitude of 17 MHz which is equivalently to a 1.7 Å separation between the unpaired electron and the proton. Such a separation is approximately equal to the nearest neighbor silicon-oxygen spacing in quartz.

TABLE II. Hyperfine and g tensor parameters for the E_4' center in crystalline SiO_2. Obtained at 20.1 GHz and 300 K.

	Principal Value	Principal Axis Direction (θ,ϕ)
g_x	2.00071	(59.6°,2.0°)
g_y	2.00076	(121.3°,71.1°)
g_z	2.00165	(46.5°,125.8°)
A_x	1.8 MHz	(98.8°,47.6°)
A_y	-0.15 MHz	(142.0°,149.1°)
A_z	52.7 MHz	(53.4°,131.0°)

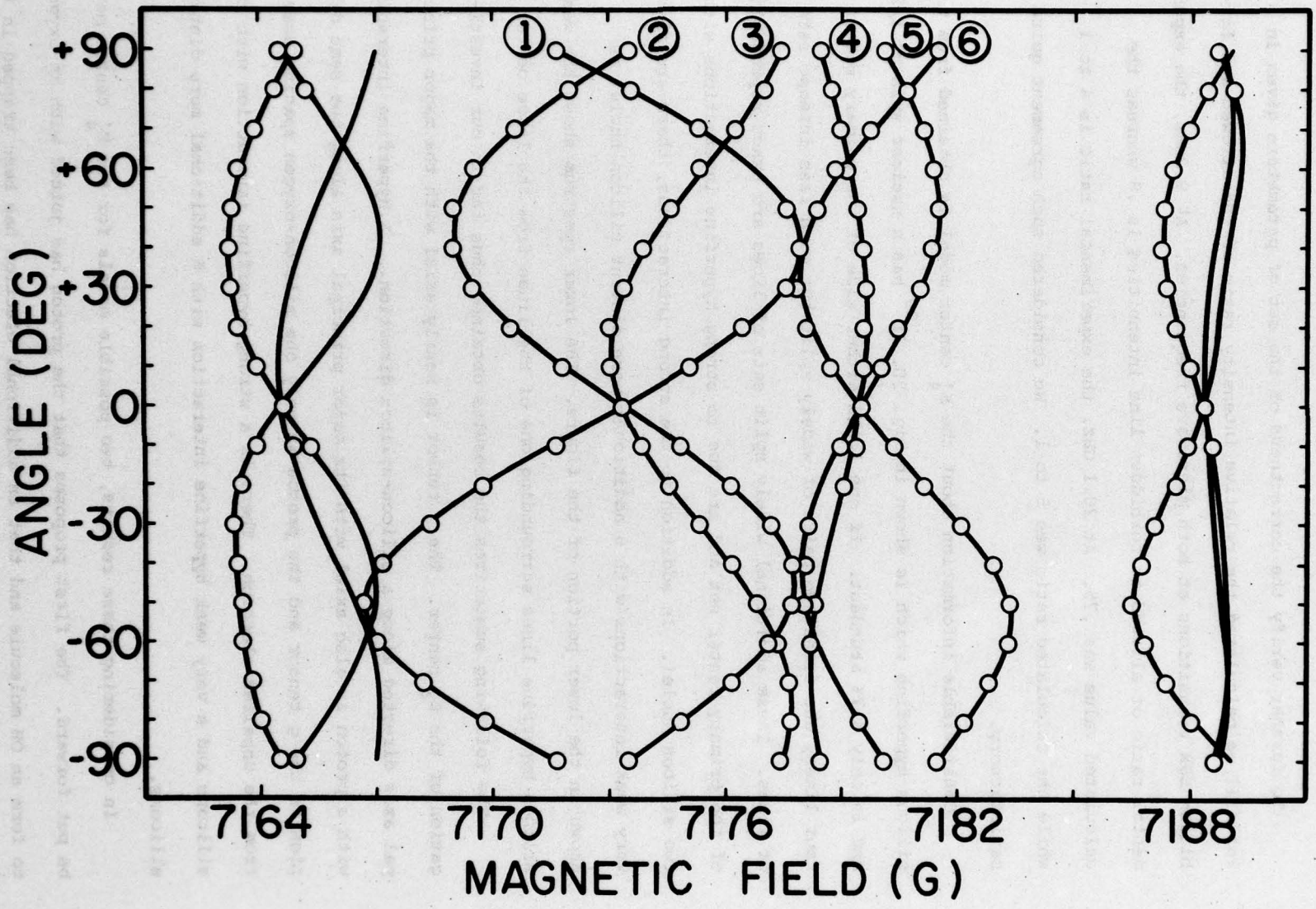

FIGURE 19. Angular dependence of E_4' center ESR spectrum.

To further verify the correctness of the set of parameters given in Table II, we calculated the relative intensity ratio of the allowed and forbidden ESR transitions at both microwave frequencies. At 9.2GHz, the experimental ratio of allowed to forbidden line intensities is .8 whereas the calculated value was .75. At 20.1 GHz, the experimental ratio is 4 to 1 while the calculated ratio was 5 to 1. We considered such agreement quite satisfactory.

Considerable information about the E_4' center model is obtained from the silicon hyperfine which is shown in Fig. 20. Si^{29} has a nuclear spin of 1/2 and is only 4.7% abundant. If one looks either side of the primary set of four lines, one finds two pairs of widely split but much less intense sets of lines. These additional widely split sets of lines are exact reproductions of the primary center set and are due to strong hyperfine interactions with two silicon nuclei. In addition to the strong interactions, there are also very weak interactions with 6 additional more distant silicon nuclei as shown in the lower portion of the figure. The lower spectrum shows the weak silicon hyperfine lines surrounding one of the lines from the large center set.

The following summarizes the results obtained thus far in our investigation of the E_4' center. The g tensor is nearly axial with the major principal axis directed along a silicon-silicon direction. A hyperfine interaction with a proton is also axial with its major principal axis along the same direction as the g tensor and the proton is only one silicon-oxygen spacing away from the unpaired electron. There is a strong hyperfine interaction with two silicons and a very weak hyperfine interaction with 6 additional more distant silicons.

In considering these results, two possible models for the E_4' center may be put forward. The first proposes that the proton has joined with an oxygen to form an OH molecule and that an additional electron has been trapped in the

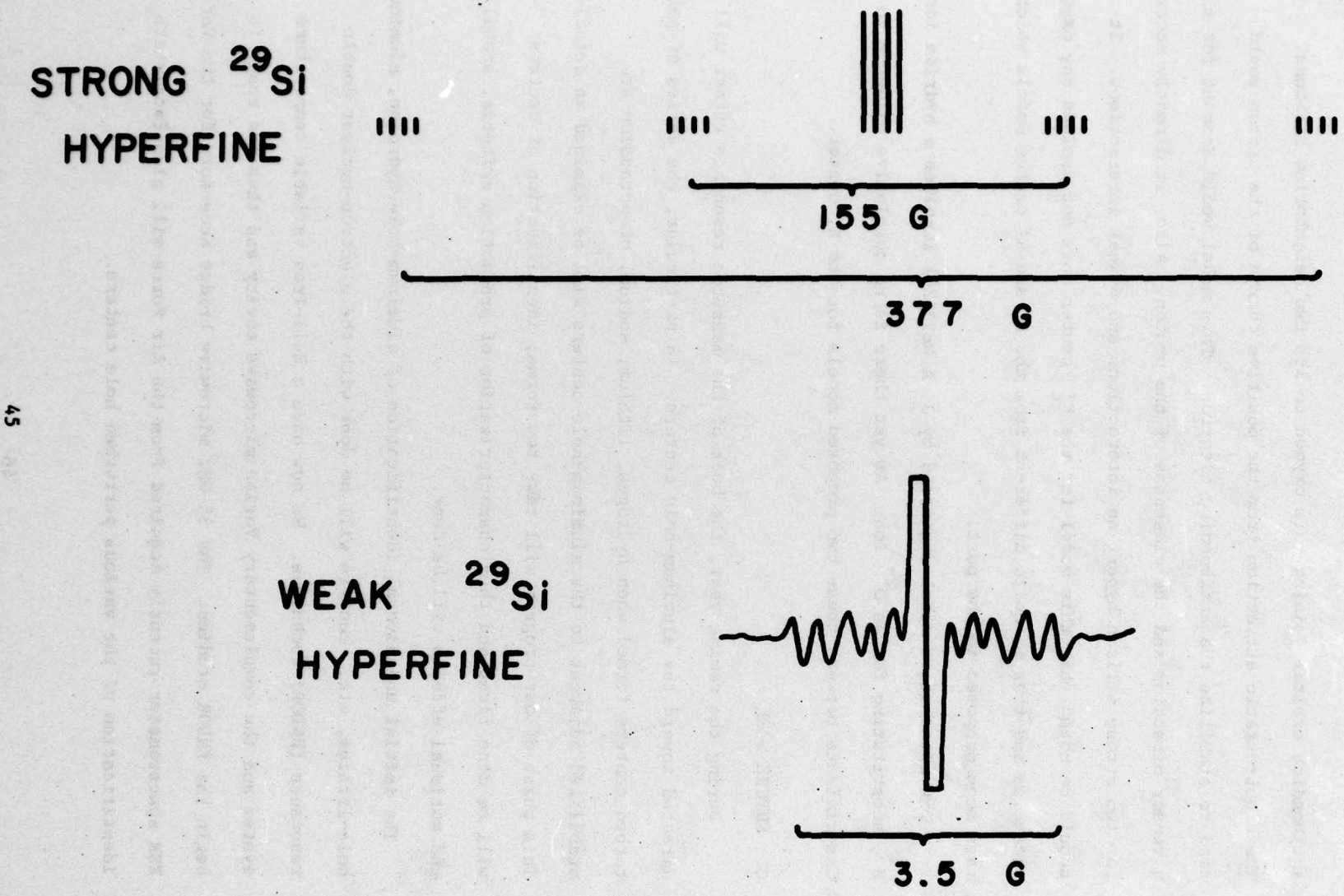

FIGURE 20. Silicon hyperfine spectra for E_4' center.

antibonding orbital joining this oxygen to its two neighboring silicons. The electrostatic attraction from the positive charge of the proton would tend to stabilize the antibonding electron. This model would account for the g tensor direction and the closeness of the proton. Also, it directly accounts for two strong silicon hyperfine interactions and 6 weak interactions. It should be noted that this model for the E_4' center does not include any oxygen vacancies and thus is quite different from the E_1' and E_2' center models which have been proposed in the past.

The alternative model suggested by J. A Weil(26) involves a hydride ion, H^-, substituting for an O^{2-} ion. As yet there is no conclusive evidence to discriminate between these two proposed models for the E_4' center.

C. FUTURE WORK

During the coming year, the bulk of the magnetic resonance effort will be directed toward the aluminum-hole centers. In particular, the series of perturbed centers formed when hydrogen, lithium, sodium, or potassium are stabilized adjacent to the aluminum-hole centers will be examined in detail. This phase of our program will take two forms; identification of centers will be done first and then characterization of production criteria, stabilities, and moticnal effects will be done.

The initial unequivocal identification of aluminum-hole-hydrogen, aluminum-hole-lithium, etc. centers will be done with the electron-nuclear double resonance (ENDOR) technique. We now have a Heli-Tran variable temperature system and the complementary Varian microwave cavity and thus are ready to begin the ENDOR studies. The 35 GHz microwave bridge accessory for the Varian ESR spectrometer recently acquired from the Air Force will also facilitate identification of the various perturbed hole centers.

The characterization of the production criteria will be aided by the ready supply of swept samples. Thermal anneal runs will be carefully repeated and attempts will be made to sort out the various decay steps observed between 130 K and room temperature in Fig. 13.

VI. REFERENCES

1. Progress Report 8 for RADC In-House Work Units 46001704 and 46001804, 1978.

2. D. B. Fraser, Physical Acoustic (W. P. Mason, ed.), Vol. V, pp. 59-110. Academic Press, New York, 1968.

3. B. S. Berry and A. S. Nowick, Physical Acoustics, (W. P. Mason, ed.) Vol. III - Part A, pp. 1-42. Academic Press, New York, 1966.

4. C. M. Zener, Imperfections in Nearly Perfect Solids (W. Schockley, J. H. Holloman, R. Maurer and F. Seitz, eds.) pp. 289-314. Wiley, New York, 1952.

5. Ref. 1 p. 95.

6. W. J. Spencer and W. L. Smith, J. Appl. Phys. 37, 2557 (1966).

7. Robert C. Dobkin, Linear Applications p. L8-8 National Semiconductor, Santa Clara, Ca 1969.

8. B. R. Capone, A. Kahan, R. N. Brown and J. R. Buckmelter, IEEE Trans on Nuc. Sci., NS17, 217 (1970).

9. C. K. Jones and C. S. Brown, Proc. Phys. Soc. (London) 82, 375 (1963).

10. R. Berman, quoted in Ref. 1 p. 98.

11. A. Kats, Phillips Res. Repts. 17, 133 (1962).

12. Gerda B. Krefft, Radiation Effects, 26, 249 (1975).

13. R. N. Brown and A. Kahan, J. Phys. Chem. Solids, 36, 467 (1975).

14. J. B. Bates and R. A. Perkins, Phys. Rev. B, 16, 3713 (1977).

15. B. Henderson and W. A. Sibley, J. Chem. Phys. 55, 1276 (1971).

16. G. Zundel, The Hydrogen Bond, Recent Developments in Theory and Experiment, Ch15 (North Holland, 1975).

17. G. E. Walrafen, Water - A Comprehensive Treatise, Vol. 1, pp. 151-214, (Plenum, N.Y. 1972).

18. J. A. Weil, Rad. Eff. 26, 261 (1975).

19. R. H. Silsbee, J. Appl. Phys. 32, 1459 (1961).

20. R. A. Weeks and C. M. Nelson, J. Am. Ceram. Soc. 43, 399 (1960).

21. R. A. Weeks, Phys. Rev. 130, 570 (1963).

22. R. A. Weeks, and M. Abraham, J. Chem. Phys. 42, 68 (1965).

23. B. D. Perlson and J. A. Weil, J. Magn. Res. 15, 594 (1974).

24. J. H. Mackey, J. Chem. Phys. 39, 74 (1963).

25. J. H. Mackey, J. W. Boss, and D. E. Wood, J. Magn. Res. 3, 44 (1970).

26. J. A. Weil, private communication.

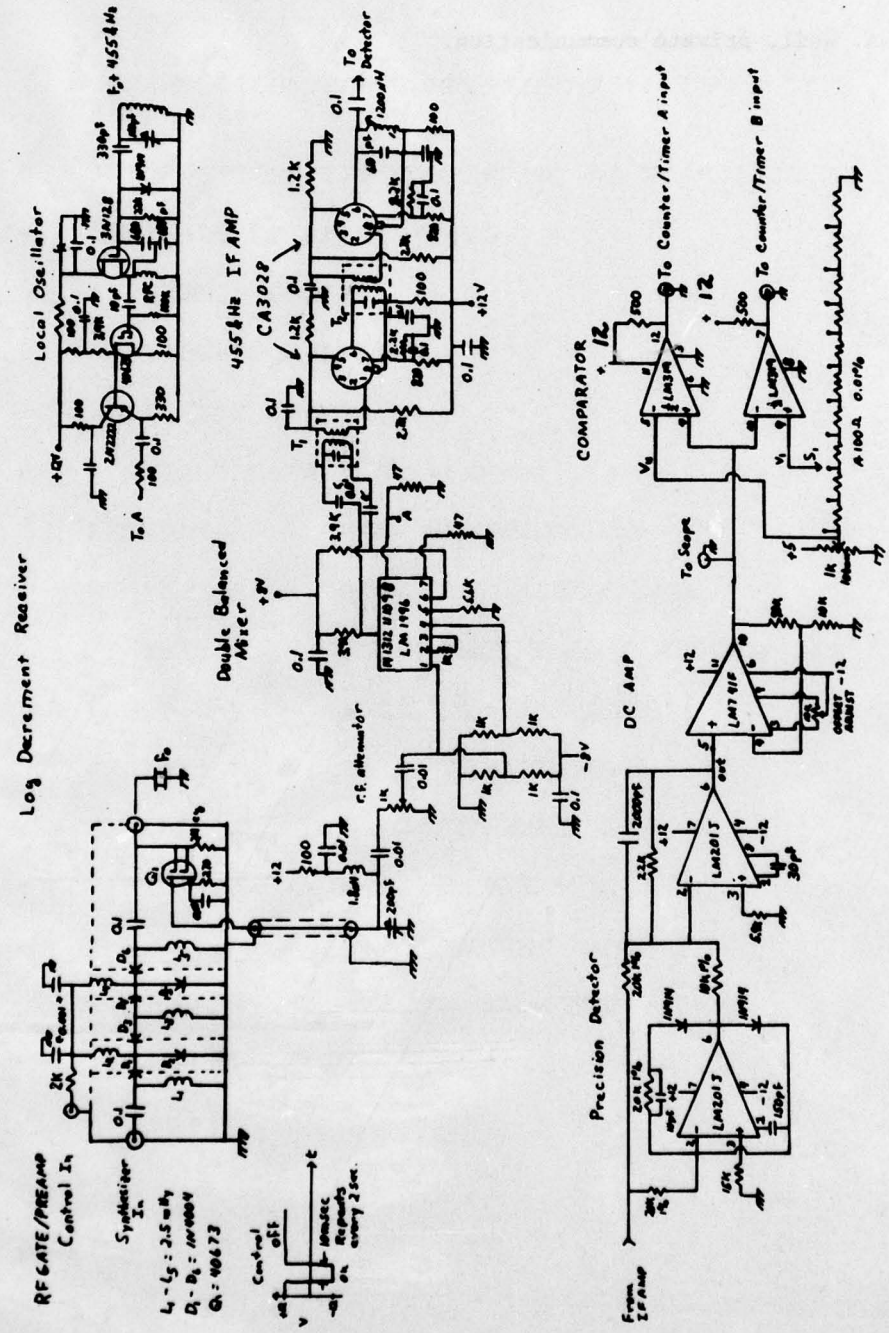

1 June 78
J J Martin

MISSION
of
Rome Air Development Center

RADC plans and conducts research, exploratory and advanced development programs in command, control, and communications (C^3) activities, and in the C^3 areas of information sciences and intelligence. The principal technical mission areas are communications, electromagnetic guidance and control, surveillance of ground and aerospace objects, intelligence data collection and handling, information system technology, ionospheric propagation, solid state sciences, microwave physics and electronic reliability, maintainability and compatibility.

Printed by
United States Air Force
Hanscom AFB, Mass. 01731